

Chapter 10

Stable Isotopes of Transition and Post-Transition Metals as Tracers in Environmental Studies

Thomas D. Bullen

Abstract The transition and post-transition metals, which include the elements in Groups 3–12 of the Periodic Table, have a broad range of geological and biological roles as well as industrial applications and thus are widespread in the environment. Interdisciplinary research over the past decade has resulted in a broad understanding of the isotope systematics of this important group of elements and revealed largely unexpected variability in isotope composition for natural materials. Significant kinetic and equilibrium isotope fractionation has been observed for redox sensitive metals such as iron, chromium, copper, molybdenum and mercury, and for metals that are not redox sensitive in nature such as cadmium and zinc. In the environmental sciences, the isotopes are increasingly being used to understand important issues such as tracing of metal contaminant sources and fates, unraveling metal redox cycles, deciphering metal nutrient pathways and cycles, and developing isotope biosignatures that can indicate the role of biological activity in ancient and modern planetary systems.

10.1 Introduction

The transition metals form a geochemically and isotopically complex and interesting group of elements clustered in the center of the periodic table. The term *transition metal*, according to the International Union of Pure and Applied Chemistry (IUPAC), refers to an element whose atom has an incomplete d sub-shell or which can give rise to cations with an incomplete d

sub-shell. As shown in Fig. 10.1, according to this definition transition metals occur in Groups 1B and 3B–8B of the periodic table, and the transition metals across the periodic table have progressively increasing d-shell electron occupancy up to a maximum of 9. A characteristic of transition metals is that they generally exhibit two or more oxidation states, which as a consequence often leads to differences in the stable isotope composition of the chemical compounds and aqueous species they form. Transition metals for which significant variation of stable isotope composition in natural materials has been demonstrated include chromium (Cr), iron (Fe), nickel (Ni), copper (Cu), molybdenum (Mo) and silver (Ag).

The above definition of *transition metal* specifically excludes the Group 2B elements zinc (Zn), cadmium (Cd) and mercury (Hg), which are often referred to as *post-transition metals*. These metals have the d shell filled and thus generally occur as cations only in the +2 oxidation state. However, it is useful to include the post-transition metals in any discussion of transition metals, as they provide interesting similarities and contrasts in chemical behavior, are subject to change in redox state either naturally (e.g. Hg) or under anthropogenic influence (e.g. Zn, Cd) and display significant variation of stable isotope composition in natural materials.

Given this broad perspective, a description of the isotope systematics of the transition and post-transition metals is given here, including general isotopic distribution, examples of processes leading to stable isotope fractionation, and chemical properties pertinent to the discussion of stable isotope variability observed in natural materials. Rather than providing a comprehensive treatment of these issues, the intent here is to provide a general understanding of how the transition metal stable isotopes behave in Earth's hydrosphere

T.D. Bullen (✉)
U.S. Geological Survey, MS 420, 345 Middlefield Road,
Menlo Park, CA 94025, USA

and atmosphere that are the venue of environmental research. Familiarity with the material in this section will help readers who are not well versed in stable isotope geochemistry to better appreciate the specific applications discussed in the later part of the chapter.

10.1.1 Chromium (Cr)

Chromium is an important trace element, particularly in ultramafic and mafic rock minerals, and is a major element in several minerals such as chromite (FeCr_2O_4) of the spinel group, uvarovite ($\text{Ca}_3\text{Cr}_2(\text{SiO}_4)_3$) of the garnet group, and crocoite (PbCrO_4). Chromium has numerous industrial applications, including use in electroplating, in leather tanning, as pigment in paint, and as an anticorrosion agent. Chromium is stable at the Earth's surface in two oxidation states: Cr^{6+} (Cr(VI)), commonly referred to as hexavalent Cr, and Cr^{3+} (Cr(III)), commonly referred to as trivalent Cr. Cr(VI) is a strong oxidant, and occurs mainly as the toxic, water-soluble oxyanions chromate (CrO_4^{2-}) and bichromate ($\text{HCr}_2\text{O}_7^{1-}$). Cr(III) is nontoxic and is insoluble in water.

Chromium has four stable isotopes: ^{50}Cr (4.35%), ^{52}Cr (83.79%), ^{53}Cr (9.50%) and ^{54}Cr (2.37%); note that for Cr and other elements discussed below that relative percentages of the isotopes are the values recommended by IUPAC to represent average terrestrial abundances. Igneous rocks have a very restricted range of $^{53}\text{Cr}/^{52}\text{Cr}$ which on average is about 0.12‰ (parts per thousand) less than that of NIST (National Institute of Standards and Technology) 979 Cr metal (Schoenberg et al. 2008). Presently the measured range of $^{53}\text{Cr}/^{52}\text{Cr}$ in natural materials is ~6‰, essentially reflecting the range measured for naturally occurring Cr(VI) in groundwater (Izbicki et al. 2008). Both inorganic and microbially mediated reduction of Cr(VI) to Cr(III) have been shown to result in isotope fractionation, with breakage of the strong Cr-O bond in chromate and bichromate appearing to be the rate limiting step (Ellis et al. 2002; Sikora et al. 2008). During reduction of Cr(VI) , the product Cr(III) formed at any step of the process is 3–4‰ lighter than co-existing remnant Cr(VI) . The fact that the oxidized species, Cr(VI) , is heavier than the reduced species, Cr(III) , is consistent with observations for other redox-sensitive elements such as selenium (Johnson et al.

2000; Johnson 2011) and mercury (Bergquist and Blum 2009; Blum 2011). While oxidation of Cr(III) to Cr(VI) is also likely to cause stable isotope fractionation (Schauble 2004), this phenomenon has yet to be rigorously demonstrated. Sorption of chromate and bichromate on Fe- and Al-oxyhydroxides has only a negligible instantaneous effect on the distribution of Cr isotopes, with preferential partitioning of light Cr isotopes onto sorption sites. Sorption effects may be magnified at reaction fronts such as the leading edge of a Cr contaminant plume in groundwater (Ellis et al. 2004).

10.1.2 Iron (Fe)

Iron is the most abundant element on Earth and the fourth most abundant element in the Earth's crust. Iron is the most widely used metal in industry, and thus is pervasive in the environment. Iron is stable at the Earth's surface in two oxidation states: Fe^{2+} (Fe(II)), commonly referred to as ferrous Fe, and Fe^{3+} (Fe(III)), commonly referred to as ferric Fe. Fe(II) is a strong reductant, is water-soluble, and is an important constituent of Fe minerals formed under reducing conditions (e.g. magnetite, siderite, pyrite). Fe(III) is only sparingly water-soluble and is an important constituent of Fe minerals formed under oxidizing conditions (e.g. ferrihydrite, goethite, hematite). Iron metal has a wide variety of applications in metallurgy such as construction of automobiles and ships, structural components of buildings, and machinery in general. Iron compounds such as Fe(III) -chloride and Fe(II) -sulfate are likewise widely used in industry for a variety of purposes. Iron plays an important role in biology and is an essential nutrient for nearly all living organisms. For example, Fe combines with oxygen to form hemoglobin and myoglobin, the two main oxygen transport proteins in vertebrates. Iron can serve as both electron donor and electron acceptor for a wide range of microorganisms, and thus Fe redox reactions have the potential to support substantial microbial populations in soil and sedimentary environments (Weber et al. 2006). Iron has been viewed as a limiting nutrient for phytoplankton growth in the oceans (Martin and Fitzwater 1988). Iron transformations and cycling processes are critical determinants of plant, forest and agricultural ecosystem function. Iron itself is generally non-toxic, but dissolved Fe(II) does impart an unpleasant taste to

water and Fe(III) staining of plumbing fixtures can be a nuisance.

Like Cr, Fe has four stable isotopes: ^{54}Fe (5.58%), ^{56}Fe (91.95%), ^{57}Fe (2.18%) and ^{58}Fe (0.30%). Igneous rocks have a very restricted range of $^{56}\text{Fe}/^{54}\text{Fe}$. Presently the measured range of $^{56}\text{Fe}/^{54}\text{Fe}$ in natural materials is ~5‰, with pyrites from Precambrian black shales spanning this range (~3.6 to +1.2‰ relative to igneous rocks; Severmann and Anbar 2009). Both inorganic and microbially-mediated oxidation of Fe(II) to Fe(III) and microbial reduction of Fe(III) to Fe(II) have been shown to result in stable isotope fractionation (Bullen et al. 2001; Balci et al. 2006; Beard et al. 1999). Perhaps most important in this regard is the experimentally and theoretically well-established isotope exchange equilibrium between Fe (II)- and Fe(III)-hexaquocomplexes of ~3‰ (Johnson et al. 2002; Anbar et al. 2005), in which the oxidized species, Fe(III), is heavier than the reduced species, Fe(II), as is the case for Cr. In addition, an important role for sorption of Fe onto mineral surfaces has been recognized, with heavy Fe species observed to populate the sorption sites after equilibrium is attained (Beard et al. 2010).

10.1.3 Nickel (Ni)

Nickel is used in many industrial and consumer products, including stainless steel and other metal alloys, coins, rechargeable batteries, and electroplating. Nickel is an important trace element in ultramafic and mafic rocks. Nickel is stable at the Earth's surface in three oxidation states: primarily as Ni^{2+} (Ni(II)), but also as Ni^{1+} (Ni(I)) and Ni^{3+} (Ni(III)). Nickel is an important enzyme cofactor, for example in urease, which assists in the hydrolysis of urea.

Nickel has five stable isotopes: ^{58}Ni (68.1%), ^{60}Ni (26.2%), ^{61}Ni (1.1%), ^{62}Ni (3.6%) and ^{64}Ni (0.9%). In a recent study of Ni stable isotope variations related to methanogenesis, Cameron et al. (2009) found that methanogens cultured in the laboratory preferentially assimilated light Ni from the media, leaving the residue enriched in heavy Ni isotopes. Fractionation of as much as 1.6‰ for $^{60}\text{Ni}/^{58}\text{Ni}$ was observed. In contrast, little variability was observed among meteorites, basalts and continental sediments, suggesting

a lithologic baseline for comparison of this potential biomarker of methanogenesis.

10.1.4 Copper (Cu)

Copper has a wide range of industrial applications, including use for electrical wires, in metal alloys, in boat paint to prevent biologic fouling, in water and gas supply pipes, and in coins. Copper is stable at the Earth's surface in two oxidation states: Cu^{1+} (Cu(I)), which is the common form in sulfide minerals such as chalcopyrite (CuFeS_2), chalcocite (Cu_2S), and enargite (Cu_3AsS_4); and Cu^{2+} (Cu(II)), which is the common form in aqueous solution. Copper can be toxic to animals, due in large part to its ability to accept and donate single electrons readily as it changes between oxidation states. This is thought to catalyze the production of reactive radical ions leading to the condition known as oxidative stress.

Cu has two stable isotopes: ^{63}Cu (69.17%) and ^{65}Cu (30.83%). In natural materials, the measured range of $^{65}\text{Cu}/^{63}\text{Cu}$ is approximately 9‰ for solid samples and 3‰ for water samples (Larson et al. 2003; Borrok et al. 2008). In one study of possible Cu stable isotope fractionation processes, abiotic oxidative dissolution of Cu-bearing sulfide minerals resulted in the product aqueous Cu(II) being ~1.4‰ heavier in terms of the $^{65}\text{Cu}/^{63}\text{Cu}$ ratio than Cu in chalcopyrite and ~3.0‰ heavier than Cu in chalcocite. Involving the microbe *Acidithiobacillus ferrooxidans* in the dissolution process reduced the fractionation observed in both cases (Mathur et al. 2005).

Copper isotopes are beginning to provide important new insights into how Cu behaves in Earth's rivers and oceans, as well as how the isotopes may be fractionated. Vance et al. (2008) reported $^{65}\text{Cu}/^{63}\text{Cu}$ ratios for riverine water, estuarine water and particulates, and open ocean water samples. They observed that dissolved Cu in rivers had $^{65}\text{Cu}/^{63}\text{Cu}$ of from 0.02 to 1.45‰ greater than that of the NIST 976 Cu standard, and for the most part greater than that of Cu in crustal rocks (+0.16‰ relative to NIST 976). In the estuarine samples, $^{65}\text{Cu}/^{63}\text{Cu}$ of dissolved Cu was 0.8–1.5‰ greater than that of Cu associated with particulate material. Vance et al. (2008) interpreted this isotopic contrast to reflect isotopic partitioning of the weathered pool of Cu between a light fraction adsorbed to

particulates and a heavy dissolved fraction dominated by Cu bound to strong organic complexes, providing a mechanism to deliver heavy dissolved Cu to the oceans. Dissolved Cu in open ocean water samples was even heavier than that in the river waters, suggesting a continuation of the fractionation between dissolved and particulate Cu fractions particularly in the surface ocean.

10.1.5 Zinc (Zn)

The post-transition metal Zn is used in electroplating, metal alloys, pigment in paint, agricultural fertilizers and pesticides, galvanized roofing material, and television-screen phosphors. Zinc is stable at the Earth's surface in one oxidation state, Zn^{2+} (Zn(II)). The large pool of Zn^0 metal produced industrially is manufactured specifically for purposes that take advantage of its high oxidation potential relative to other metals (e.g. as an anti-fouling and anti-corrosive agent on the submerged portion of ship hulls and propeller shafts). Zinc is an important enzyme cofactor, for example in alcohol dehydrogenase in humans, and is generally thought to be non-toxic.

Zinc has five stable isotopes: ^{64}Zn (48.63%), ^{66}Zn (27.90%), ^{67}Zn (4.10%), ^{68}Zn (18.75%) and ^{70}Zn (0.62%). In natural materials, the measured range of $^{66}Zn/^{64}Zn$ is approximately 2‰ (Cloquet et al. 2008). Maréchal et al. (1999) published the first high-quality measurements of zinc and copper isotope compositions in a variety of minerals and biological materials. Since this pioneering work the field of Zn isotope biogeochemistry has rapidly expanded into a variety of environmental applications. For example, Zn has a relatively low boiling point (~910°C) compared with that of Cr or Cu, within the operating temperature range of ore smelters. Thus Zn can evaporate from ore during smelting, which would favor escape of light Zn isotopes in the exhaust as demonstrated by Mattielli et al. (2009), and retention of heavy Zn isotopes in the slag residue as shown by Sivry et al. (2009). Kavner et al. (2008) demonstrated that electroplated Zn, reduced to metallic state from a large pool of aqueous Zn(II), is isotopically light compared to the parent solution, potentially resulting in a large pool of isotopically light electroplated Zn in the environment. In addition, Weiss et al. (2007) demonstrated

that Zn adsorption due to complexation by organic compounds is selective for the heavy Zn isotopes, resulting for example in peat samples that have heavier Zn isotope compositions than any potential natural source. On the other hand, Borrok et al. (2008) pointed out that Zn uptake by microorganisms is selective for the light Zn isotopes. Thus there are several fractionation processes for Zn that might modify its isotope composition in the environment.

10.1.6 Molybdenum (Mo)

Molybdenum is used in the production of high-strength steel alloys, as pigments and catalysts, and in a variety of high temperature applications such as lubricants, electrical contacts and industrial motors. Molybdenum is stable at the Earth's surface in several oxidation states, the most stable being Mo^{4+} (Mo(IV)) and Mo^{6+} (Mo(VI)). Molybdenum is an essential enzyme cofactor in nearly all organisms, with particular importance for nitrogen fixation, nitrate reduction and sulfite oxidation. Molybdenum is soluble in strongly alkaline water such as seawater, forming molybdates (MoO_4^{2-}). Molybdates bear structural similarities to chromates, yet are weaker oxidants. In fact, although Mo lies directly below Cr in the periodic table, Mo compounds show more similarity to those of tungsten (W), which lies directly below Mo in the periodic table.

Molybdenum has seven stable isotopes: ^{92}Mo (14.84%), ^{94}Mo (9.25%), ^{95}Mo (15.92%), ^{96}Mo (16.68%), ^{97}Mo (9.55%), ^{98}Mo (24.13%) and ^{100}Mo (9.63%). In natural materials, the measured range of $^{97}Mo/^{95}Mo$ is ~3‰, with pelagic clays extending to -1‰ and suboxic sediment pore fluids extending to +2‰ relative to a modeled “bulk earth” composition as defined by Mo ores (Barling et al. 2001; Siebert et al. 2003; Anbar 2004; Arnold et al. 2004). Molybdenum isotopes are fractionated during adsorption to ferromanganese oxides in oxidizing environments (Barling et al. 2001; Barling and Anbar 2004) and precipitation of Fe-Mo-S solids in reducing environments (Poulson et al. 2006; Neubert et al. 2008), and the extent of fractionation differs in these two extreme conditions. Thus Mo isotopes can provide information about local redox conditions.

10.1.7 Cadmium (Cd)

The post-transition metal Cd is used primarily in Ni-Cd batteries, metal alloys, electroplating, pigment in paint, and electronic components. Cadmium is stable at the Earth's surface primarily in the Cd²⁺ (Cd(II)) oxidation state. Cadmium has a strong geological affinity to Zn, but unlike Zn can be toxic to humans due to its effective substitution for calcium in bone and its tendency to concentrate in the kidneys and liver where it may become carcinogenic.

Cadmium has eight stable isotopes: ¹⁰⁶Cd (1.25%), ¹⁰⁸Cd (0.89%), ¹¹⁰Cd (12.49%), ¹¹¹Cd (12.80%), ¹¹²Cd (24.13%), ¹¹³Cd (12.22%), ¹¹⁴Cd (28.73%) and ¹¹⁶Cd (7.49%). In terrestrial materials, the measured range of ¹¹⁴Cd/¹¹⁰Cd is approximately 0.5‰; considering anthropogenically influenced materials extends that range to ~1.5‰ (Ripperger and Rehkämper 2007; Schmitt et al. 2009a, b; Shiel et al. 2010). Cadmium has an even lower boiling point (~760°C) than Zn, and like Zn, Cd in ores likely evaporates during smelting favoring escape of light Cd isotopes in the exhaust, as recently demonstrated by Cloquet et al. (2006a). Cadmium behaves like Zn during electroplating (Kavner et al. 2008), potentially resulting in a large pool of isotopically light Cd in the environment. Although Cd is discussed in this chapter mainly in a multi-tracer context, Rehkämper et al. (2011) provide a thorough discussion of the application of Cd isotopes in environmental studies.

10.1.8 Mercury (Hg)

The post-transition metal Hg is used in thermometers and other scientific apparatus, amalgam for dental restoration, Hg vapor lamps, cosmetics, and liquid mirror telescopes. Historically, Hg has been widely used in gold mining operations. Mercury is stable at the Earth's surface as soluble Hg²⁺ (Hg(II)) and as Hg⁺ (Hg(I)) in the form of monomethylmercury (CH₃Hg⁺). In addition, and unlike the other transition and post-transition metals, Hg has a stable gaseous form (Hg⁰) at environmental temperatures with a residence time in the atmosphere of approximately 1 year (Schroeder and Munthe 1998). Mercury and its compounds (e.g. monomethylmercury (MeHg), mercuric chloride) are

extremely toxic and can be readily ingested through inhalation or absorption through the skin and mucous membranes.

Mercury has seven stable isotopes: ¹⁹⁶Hg (0.15%), ¹⁹⁸Hg (9.97%), ¹⁹⁹Hg (16.87%), ²⁰⁰Hg (23.10%), ²⁰¹Hg (13.18%) ²⁰²Hg (29.86%) and ²⁰⁴Hg (6.87%). Based on the compilation of existing high-precision Hg isotope data reported by Bergquist and Blum (2009), the measured range of ²⁰²Hg/¹⁹⁸Hg in natural materials resulting from *mass dependent fractionation* (MDF) between coexisting Hg pools is approximately 7‰. This is remarkable, considering that measurable fractionation of Hg isotopes was generally thought to be non-existent as late as the 1990s. In addition, Hg stable isotopes exhibit considerable *mass independent fractionation* (MIF), in which the odd-numbered isotopes ¹⁹⁹Hg and ²⁰¹Hg behave differently than the even-numbered isotopes in certain chemical reactions such as photochemical reduction (Bergquist and Blum 2007), leading to significant enrichments and depletions of the odd-numbered isotopes relative to the even-numbered isotopes in environmental Hg pools.

Although Hg is included in the discussion here, Blum (2011) provides a thorough discussion of the theory and application of Hg isotopes in environmental studies. In his chapter, Blum (2011) points out that most environmental applications of Hg isotopes are concerned with either (1) interpreting the isotopic composition of MeHg occurring in sediments and organisms, or (2) interpreting the isotopic composition of Hg(II) associated with sediments or deposited onto the land surface or into a water body. In addition, the author stresses the importance of redox reactions as the main cause of isotope fractionation in the Hg system and the role that the isotopes can play in helping to increase our understanding of the chemical bonding environments that lead to various Hg fractions in sediments and other natural materials.

10.1.9 Other Transition Metals Potentially Having Useful Isotopic Variability

There are several other transition metals, outlined in blue in Fig. 10.1, that have multiple stable isotopes and thus the potential for stable isotope variability in

3B	4B	5B	6B	7B		8B	1B	2B
Sc scandium	Ti titanium	V vanadium	Cr chromium	Mn manganese	Fe iron	Co cobalt	Ni nickel	Cu copper
Y yttrium	Zr zirconium	Nb niobium	Mo molybdenum	Tc technetium	Ru ruthenium	Rh rhodium	Pd palladium	Cd cadmium
(La) lanthanum	Hf hafnium	Ta tantalum	W tungsten	Re rhenium	Os osmium	Ir iridium	Pt platinum	Au gold

Fig. 10.1 A portion of the Periodic Table of the Elements, showing the transition and post-transition metals. Elements with *green borders* are those for which significant variability of stable isotope composition has been observed in natural materials. Elements with *blue borders* are those that have

nature, but which have yet to be rigorously explored in terms of isotope systematics. Examples of these elements that would be especially useful in environmental studies are titanium (Ti), vanadium (V), silver (Ag), tungsten (W) and rhenium (Re). For example, as pointed out by Severman and Anbar (2009), Re (^{185}Re (37.4%), ^{187}Re (62.6%); common oxidation states Re^{2+} , Re^{4+} , Re^{6+} , Re^{7+}) is removed from solution into sediments only under anoxic or suboxic conditions, making it a suitable tracer for moderately reducing conditions. In contrast, V (^{50}V (0.25%), ^{51}V (99.75%); common oxidation states V^{2+} , V^{3+} , V^{4+} , V^{5+}) is scavenged from solution by manganese oxides and Fe-oxyhydroxides, making it a suitable tracer for oxic conditions. Both potential redox-tracing applications assume that sedimentation promotes isotope fractionation between sediment and residual aqueous pools of Re or V, but such fractionation has yet to be demonstrated.

Silver, in addition to its historic value as a precious metal, is widely used in dentistry, photographic materials, mirrors and optics, control rods in nuclear reactors, clothing (as an anti-fungal agent) and in certain medicines. Silver has the highest electrical conductivity of any element and the highest thermal conductivity of any metal and thus is widely used in electrical contacts and conductors. Silver is stable at the Earth's surface primarily in three oxidation states: Ag^0 or native silver, and Ag^{+1} and Ag^{+2} , the common forms

more than one stable isotope and thus the potential to have variability of stable isotope composition in natural materials, but such variability has yet to be rigorously demonstrated. Elements with *red borders* have only one stable isotope (no stable isotope in the case of Tc)

in a wide variety of Ag-containing compounds and minerals. Silver has two stable isotopes: ^{107}Ag (51.84%) and ^{109}Ag (48.16%). In an initial study of Ag stable isotope variation in sediment and domestic and industrial sludge samples, Luo et al. (2010) reported a small but significant range of variation in $^{109}\text{Ag}/^{107}\text{Ag}$ of 0.1‰ that bracketed the value for their standard. They found a different value for Ag from a fish liver (+0.28‰ relative to their standard) that may indicate a biological influence. However, at this stage Ag is only beginning to be explored in terms of stable isotope variability.

Tungsten provides an especially intriguing but as yet untested candidate for stable isotope variation in natural materials at the Earth's surface. Tungsten is used in many high-temperature applications, such as light bulbs and welding processes, and in lubricants, abrasives, ceramic glazes, and heavy metal alloys. The most common oxidation state of W at the Earth's surface is W^{6+} , but W exhibits all oxidation states from W^{2-} to W^{6+} . Tungsten has five stable isotopes: ^{180}W (0.12%), ^{182}W (26.50%), ^{183}W (14.31%), ^{184}W (30.64%) and ^{186}W (28.43%); ^{180}W is radioactive, but with a half-life of 1.8×10^{18} years it is essentially stable. While there is substantial literature describing ^{182}W variations in meteorites, there have been essentially no published systematic studies of low-temperature processes involving W. However, Irisawa and Hirata (2006) reported that W isotope ratios for

sediment reference materials differed significantly from values for igneous rocks, hinting at the possibility that low-temperature redox and/or sorption processes may fractionate the W isotopes.

The potential for Ti to have significant variability of stable isotope composition in natural materials at the Earth's surface is probably less than that for W, V and Re. This is due to the fact that the geochemistry of Ti is dominated by the Ti^{4+} oxidation state, and Ti is not known to play a large role in biological processes such as enzyme stabilization. Regardless, titanium has five stable isotopes spanning a large mass range: ^{46}Ti (8.0%), ^{47}Ti (7.3%), ^{48}Ti (73.8%), ^{49}Ti (5.5%) and ^{50}Ti (5.4%). If our experience with exploration of stable isotope variability of other elements dominated by a single oxidation state may serve as a guide, it is not unrealistic that a thorough reconnaissance study of Ti or other unexplored transition metal stable isotope systematics in environmental materials (e.g. nanoparticles, pigments, electroplated steel) would reveal unexpected surprises.

10.2 Methodology

Although the transition and post-transition metals represent a geochemically diverse group of elements, the details of the analytical procedures required for measurement of their isotope compositions are quite uniform. Once a laboratory establishes a protocol for analysis of one of these metals, it can be relatively straightforward to add more of the remaining metals to the repertoire. On the other hand, transition and post-transition metals are everywhere, in field and laboratory equipment, and care must be taken to maintain strict cleanliness during sample collection, processing and measurement.

10.2.1 Sampling Protocols

As a general rule, the sampling protocol for transition or post-transition metal isotope analysis of water is identical to that for standard dissolved cation analysis. The sample is collected using plastic tubing for pumps or plastic containers for dipping and placed into plastic containers that have been rinsed several times with the

water being collected. Pre-cleaning of the plastic containers with nitric acid may be required if container "blanks", obtained by allowing distilled water to sit in the container for an extended period of time, reveal significant metal content. The sample needs to be filtered, the pore-size of the filter being determined by the question being asked (e.g. is there isotopic fractionation between colloidal and non-colloidal size fractions?). Generally an in-line filter with 0.1 μm pore size provides sufficient filtration, but this may cause retention of some of the colloidal fraction as well (size: 1 nm–1 μm). Alternatively, the sample can be filtered after initial collection using a plastic syringe fitted with a disposable filter cartridge. Care must be taken to prevent possible redox changes of the redox-sensitive species in the oxic environment. Use of an in-line filter minimizes potential formation of Fe- and Mn-oxyhydroxides that can scavenge the metals from solution. Additionally, collection and filtration can be carried out in a portable nitrogen-atmosphere glove box. The sample should be acidified with exceptionally clean nitric or hydrochloric acid, to a pH of approximately 2.0. Additional precautions such as wearing ultra-clean over-garments, gloves and boots may be required, particularly when metal concentrations are expected to be extremely small.

Knowledge of metal concentrations in the sample prior to collection for isotope analysis is useful in order to ensure that sufficient metal is collected to meet the requirements of the analytical technique. As a general rule of thumb, sufficient material to provide 1–10 μg of the target metal should be collected when possible. The amount of metal required for isotope analysis ranges from as little as 5 ng to as much as 1 μg , depending on factors such as ionization efficiency in the mass spectrometer and resolution mode employed (see below). Moreover, knowledge of procedural blank levels is useful for deciding what kinds of plastic tubing and containers to use and what protective measures to take. A worthwhile exercise is to take a supply of the cleanest distilled laboratory water available to the field site and to treat the distilled water as a sample, using all intended plastic tubing and containers, filters and other collection equipment, and techniques. One or two field blanks should be collected during each sampling session, and the blank should be measured for concentration of the metal of interest prior to investing time in sample preparation and mass spectrometry.

Collection of solid samples such as soils, plant tissues and landfill materials requires common sense more than anything. Solid samples should be collected into plastic bags, and care should be taken to ensure that sampling equipment (e.g. shovels, augers, stem-wood borers) do not contain the metal of interest. Particular care should be taken to avoid sampling equipment with painted surfaces as the paint is likely to have transition or post-transition metals as pigments.

10.2.2 Sample Preparation

Prior to mass spectrometry, the metal of interest must be isolated from the rest of the sample matrix and particularly from elements that would produce isobaric interferences on the target masses for analysis. For example, in preparing a sample for Cr isotope analysis, all Ti, V and Fe must be removed, as each of these metals has an isotope at the same mass as a Cr isotope. Similarly, some elements form double-charged ions in the mass spectrometer that are detected at $\frac{1}{2}$ of their mass due to the direct dependence of ion flight path through the magnetic sector of the mass spectrometer on mass:charge ratio of the ion. For example, Ba^{2+} ions can be formed in both multi-collector inductively coupled plasma mass spectrometry (MC-ICP-MS) and thermal ionization mass spectrometry (TIMS), the two common methods for analysis of metal stable isotope composition. $^{132}\text{Ba}^{2+}$ would be detected at mass 66, $^{134}\text{Ba}^{2+}$ would be detected at mass 67, and $^{136}\text{Ba}^{2+}$ would be detected at mass 68, all directly overlapping the Zn isotopes of the same masses. Thus, a goal of the chemistry is to produce as pure a target metal fraction as possible, preferably if not assuredly with quantitative recovery.

Most chemical procedures for purification of the transition and post-transition metals involve some form of ion exchange chromatography, making use of different affinities of the metals for the ion exchange resins in different strengths of acid media. For example, Wombacher et al. (2003) developed a method to purify Cd from geological materials and meteorites. The digested sample is dissolved in 3 M HCl and loaded directly onto an exchange column containing AG1-X8 strong acid anion exchange resin. The column is rinsed with set volumes of 0.5, 1, 2 and finally

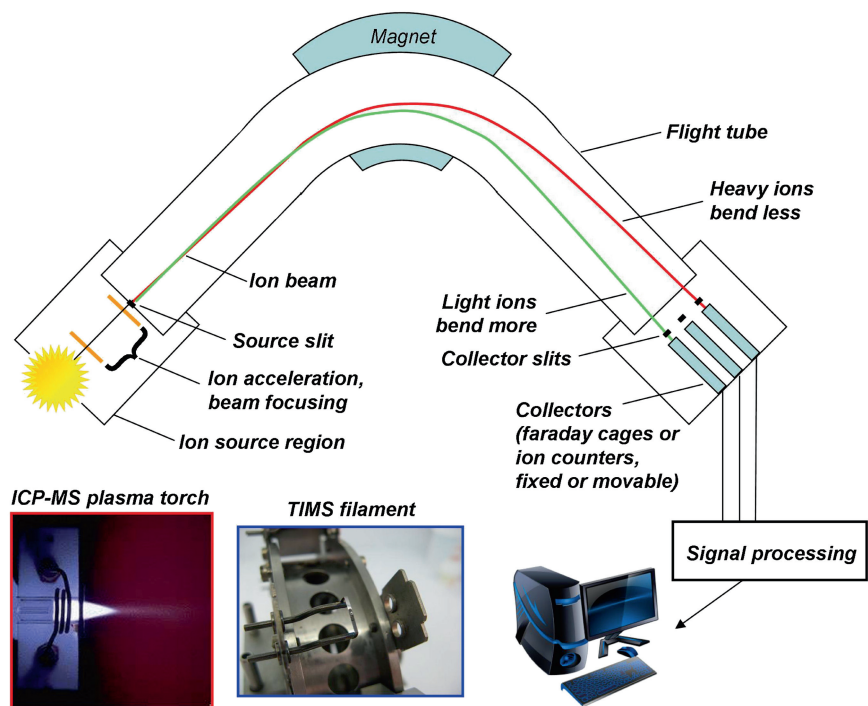
8 M HCl in order to remove the majority of matrix elements. Following this series of rinses, all that remains on the resin are Ag, Zn, tin (Sn) and Cd. Additional rinsing with 8 M HCl removes the Ag, which can be retained for isotope analysis if desired (although quantitative recovery must be demonstrated). The rinse solution is then changed to a 0.5 M HNO_3 –0.1 M HBr mixture, which removes Zn and some of the Sn from the column; this fraction can be retained for further processing for Zn isotope analysis, if desired. The rinse solution is then changed to 2 M HNO_3 , which removes the Cd and the remainder of the Sn. This product solution is then taken to dryness, re-dissolved in 6 M HCl and loaded onto a small column containing a resin (TRU Spec, Eichrom Industries) that retains the Sn but not the Cd, which is collected in a beaker. The product solution contains only Cd, and is ready for isotopic determination. This example demonstrates the versatility of the ion exchange resin method, and new element-specific resins are continually being developed as the need for new applications is encountered.

Procedures for chemical purification of the other transition and post-transition metals follow a similar logic and most are able to achieve quantitative recovery, thereby avoiding isotope fractionation on the resin column which has been demonstrated to occur for several elements such as Fe (Anbar et al. 2000). References providing detailed descriptions of purification techniques for the transition and post-transition metals discussed here include: Cr, Ellis et al. (2002; supplementary material); Fe, Beard and Johnson (1999); Ni, Cameron et al. (2009); Cu and Zn, Borrok et al. (2007); Mo, Barling et al. (2001); Cd, Wombacher et al. (2003); Ag, Luo et al. (2010); Ti, Das and Pobi (1990); V, Pelly et al. (1970); W, Sahoo et al. (2006); Re, Liu et al. (1998). Note that sample preparation of Hg for isotope analysis requires an entirely different approach, as discussed in Blum (2011).

10.2.3 Instrumentation

As mentioned above, the stable isotope composition of the transition and post-transition metals is measured using either MC-ICP-MS or TIMS. A generalized schematic of these mass spectrometers is given in Fig. 10.2, which illustrates essential aspects of their

Fig. 10.2 Generalized schematic of the important aspects of multi-collector mass spectrometers used for determination of metal stable isotope compositions. Key features are discussed in the text. Modified after Bullen and Eisenhauer (2009)



function (Bullen and Eisenhauer 2009). All instruments consist of three main components: ion source, ion optics (ion acceleration, ion beam focusing, isotope mass separation) and ion collection. Ions are produced by thermal processes in the source region: in MC-ICP-MS, the sample is injected into the source region either as a nebulized liquid aerosol or as ablated solid particulate in a gaseous stream which passes through a high-temperature plasma (up to 10,000°K; see photo insert in Fig. 10.2) at near-atmospheric pressure. At this high temperature, atoms of the sample material are very efficiently ionized. In TIMS, the sample is deposited on a wire filament (see photo insert in Fig. 10.2), placed in a high vacuum ($\sim 10^{-8}$ torr), and the filament is heated to the temperature required for ion production of the particular element (typically 800–1,700°C). The ions produced in either instrument then enter the optics region, where they are accelerated through a large potential (up to 10 kV) and focused electronically to create a discrete ion beam. In MC-ICP-MS, the vacuum must be substantially improved over this short optics region via efficient mechanical and electrical “ion getter” vacuum pumps. Beyond the ion optics region, an exceptional vacuum ($\sim 10^{-8}$ torr) must be maintained in both instruments.

The accelerated and focused ion beam then passes through a slit into the flight tube where the different isotopes of the element are dispersed by mass using an electromagnet. The width of the slit determines the ability of the mass spectrometer to partially resolve sample ions and extraneous molecules of nearly similar mass (“isobaric interferences”). For example, since the plasma in ICP-source instruments is predominantly composed of Ar, a narrow slit must be used to resolve ^{56}Fe from $^{40}\text{Ar}^{16}\text{O}$. In TIMS instruments, ^{56}Fe must be resolved from organic molecules with mass ~ 56 atomic mass units. In general, a narrower slit provides greater resolving power but reduced signal intensity.

The fundamental power of MC-ICP-MS and TIMS instruments to disperse the isotopes of an element rests in the ability of the magnet to differentially divert the flight paths of the various isotopes according to their individual energies. The ion flight paths are bent along the axis of the flight tube depending on the ratio of ion mass to charge: light ions are bent more (green path in diagram), heavy ions are bent less (red path in diagram). For any particular isotope, a restricted range of ion energies leaving the magnetic sector is required to create a concentrated, flat-topped signal that is ideal

for detection and measurement. In TIMS, ions of a particular isotope produced at the source filament are essentially mono-energetic, and once the ion beam is focused in the source region mass (i.e. energy) dispersion can be effectively achieved in the magnetic sector. In contrast, in MC-ICP-MS ions of a particular isotope leave the source region having a fairly wide energy distribution due to numerous processes occurring in the source region. Thus in most MC-ICP-MS instruments, the poly-energetic ion beam must first pass through an electrostatic discriminator (not shown) which disperses the ion beam in exactly the opposite sense to that which follows in the magnetic sector. As a result of exacting electromechanical design, the ion beam that ultimately passes out of the magnetic sector has a balanced and much smaller energy spread that allows the flat-topped signal to develop. In a few MC-ICP-MS instruments, the ion beam first passes through a “collision cell” containing molecules of a gas such as Ar where collisions of the metal ions with the gas molecules substantially reduce the kinetic energies of those ions, which can then be reaccelerated in a nearly mono-energetic condition for passage through the magnetic field as in TIMS.

Ion detection collectors are configured to perfectly intersect the resulting flight paths of the component isotope ion beams of the element. In some instruments, collectors can be moved perpendicularly to the ion paths until desired coincidence is achieved for a particular element. In other instruments, the collector positions are fixed and the trajectories of the ion beams themselves are adjusted along the final section of the flight tube by further electronic focusing in order to achieve coincidence. Collectors are either Faraday cages, credit-card sized, thin rectangular boxes open on one narrow end to receive and trap ions on the internal surfaces resulting in a measurable total ion current on the internal surfaces, or ion counters that record individual ion collisions with the counter surfaces. Faraday cages may have slits positioned along the ion flight path prior to the point of ion entry into the cage in order to better shape the ion beam for optimum signal detection. Channel-specific total ion currents detected over a certain period of time are then processed through a series of electronic conversions into signals that can be interpreted by computer software as relative isotope abundances for the element.

Each instrument has its advantages in certain applications, but as a general rule the stable isotope

composition of all the transition and post-transition metals discussed in this chapter can be most efficiently determined using MC-ICP-MS. The high ionization efficiency of the plasma source used to generate ions in MC-ICP-MS compared to that of the metal filament source used in TIMS results in improved isotope measurement of very small quantities (i.e. tens of nanograms) of elements with high ionization potentials, such as Zn (e.g. Chen et al. 2008), Mo (e.g. Barling and Anbar 2004), and Hg (e.g. Blum and Bergquist 2007). In addition, MC-ICP-MS instruments typically have the capability to sufficiently resolve measureable portions of metal ion beams from “isobaric” polyatomic interfering species having nearly the same mass (e.g. ^{56}Fe vs. $^{40}\text{Ar}^{16}\text{O}$ generated in the Ar plasma). Some interfering species, primarily oxides, can also be removed from the ion stream to a large extent by desolvating the sample prior to introduction to the plasma. Alternatively, in some instruments polyatomic molecules can be disaggregated in the collision cell apparatus described above due to collisions of the molecules with atoms of the gas supplied to the cell. In MC-ICP-MS, uncertainty due to signal noise resulting from the inherent instability of the plasma source is eliminated by measuring all ion beams simultaneously with the multicollector array. An additional strength of MC-ICP-MS is that samples can be introduced using laser ablation equipment, in which layers of atoms are sputtered off the surface of a solid material and transported by a gas stream to the plasma for ionization. Excellent references on the general topic of isotope analysis by MC-ICP-MS are Albarède and Beard (2004), Rehkämper et al. (2004) and Wieser and Schwieters (2005).

On the other hand, TIMS has been used for more than 50 years and has long been the workhorse for metal isotope research. TIMS provided much of the data on transition and post-transition metal stable isotope systematics prior to the proliferation of MC-ICP-MS in research labs and continues to provide excellent isotope measurements for more readily ionized elements such as Cr (e.g. Ellis et al. 2002) and Fe (Bullen and Amundson 2010) and even for elements that are difficult to ionize such as Cd (Schmitt et al. 2009a, b). TIMS is less affected by isobaric interferences than MC-ICP-MS because there is no need for the Ar gas and because the sample is ionized under high vacuum rather than in an aqueous solution or gas stream at atmospheric pressure. TIMS likewise benefits from

simultaneous multicollector ion beam detection (Fantle and Bullen 2009). Typical external precision (i.e. comparison of total procedural replicates for natural samples) is at the 0.1‰ level for both TIMS and MC-ICP-MS. A disadvantage of both instruments is a sizable footprint in the laboratory and high costs for purchase and maintenance.

10.2.4 Data: Acquisition, Reduction, Accuracy, and Standard Reference Materials

Isotope fractionation of the ion beam produced in both TIMS and MC-ICP-MS, which is an unavoidable characteristic of both analytical platforms, means that the relative proportion of isotopes of an element reaching the detectors in the mass spectrometer is not identical to that of the sample. This instrument-induced fractionation, or “mass bias”, is often larger than the isotopic variation between samples. In MC-ICP-MS, light ions of any element are preferentially discriminated against and removed from the ion stream at the sampling cones situated just beyond the plasma source, resulting in relatively heavy raw measured ratios that tend to stay very constant over the course of a measurement. In TIMS, light ions of any element are preferentially ionized off the filament surface, causing the raw measured ratio to be light at the outset and progressively heavier over the course of a measurement. Thus it is essential to provide some means to correct for isotope discrimination so that measured isotope compositions of samples can be compared to those of standards and other samples.

The classic approach to correct for isotope discrimination in TIMS is referred to as the *double spike technique*. An excellent treatment of the theoretical aspects of the double spike technique is given by Johnson and Beard (1999), and a practical overview of the technique is provided by Rudge et al. (2009). This technique requires that the element have at least four naturally-occurring isotopes, two that can be used as isotopes for the double spike and two that can be used to calculate a ratio that provides information on the relative natural isotope composition of a sample. The double spike is a mixture of two typically minor isotopes of the element that have each been

industrially enriched in their proportion relative to the other isotopes. There are now several commercial suppliers of highly enriched (i.e. typically >90% pure) stable isotopes of most multi-isotopic elements, and thus it is relatively straightforward to create a double spike using any combination of two isotopes of an element. The double spike mixture, which has been carefully characterized for isotope composition and concentration, is added to a sample prior to analysis thus imparting an unnatural isotope composition to the sample-double spike mixture. Following analysis, the measured ratio of the two isotopes used to create the double spike can be compared to the known, carefully characterized value to obtain a “mass bias factor” that quantifies isotope fractionation that has occurred during analysis. The measured isotope composition of the sample-double spike mixture can then be corrected based on this mass bias factor, and the double spike component of the mixture can be mathematically subtracted from the fractionation-corrected composition to reveal the natural ratios of the two or more isotopes not used for the double spike as the residual.

For example, the $^{53}\text{Cr}/^{52}\text{Cr}$ natural isotope ratio of a sample can be determined using a double spike consisting of a mixture of nearly pure ^{50}Cr and ^{54}Cr , the two minor isotopes of Cr. Of the elements discussed here, Cr, Fe, Ni, Zn, Cd, Mo, Hg, Ti, and W are suitable for analysis by the double spike technique while Ag, Re and V are not. An important advantage of the double spike technique is that the double spike solution can be added to the sample prior to purification chemistry, and thus, without any additional effort, can be used to correct for isotope fractionation that might occur during chemical purification prior to analysis (e.g. due to non-quantitative recovery of the metal from the resin).

The nature of MC-ICP-MS allows application of two additional techniques for correction of isotope discrimination in the instrument during analysis, *standard-sample-standard bracketing* and *internal standardization*. As the name implies, in standard-sample-standard bracketing a standard solution is analyzed directly before and after a sample, and the interpolated isotope ratio of the standard at the time of the sample analysis is taken as the reference value. This is an incredibly straightforward approach, but assumes that the sample and standard behave similarly in the plasma (e.g. have identical matrices). With internal standardization, an element with a known

isotope composition and similar fractionation behavior to the element being analyzed is added to the sample solution prior to aspiration into the plasma (e.g. Zr as an internal standard for Mo isotope analysis, Cu as an internal standard for Fe or Zn isotope analysis). The isotope ratio measured for the internal standard can be compared to its known value to quantify machine-induced fractionation and a correction can then be applied to the isotope ratio of the target element on a scan by scan basis. Using internal standardization, a plot of the measured isotope ratios of the target element vs. those of the internal standard element typically defines a mass dependent fractionation relationship that provides the basis for the correction (Longerich et al. (1987); Maréchal et al. (1999).

The power of the standard-sample-standard bracketing and internal standardization techniques is that they can be used for isotopic analysis of any element having two or more isotopes. On the other hand, the double spike technique required for TIMS stable isotope analysis can likewise be used for MC-ICP-MS isotope analysis of elements having four or more isotopes, and is in essence a special case of internal standardization. The advantage of using a double spike for MC-ICP-MS analysis is that quantitative yield during sample purification is not required as it is for standard-sample-standard bracketing and internal standardization approaches (Siebert et al. 2001).

Differences in transition and post-transition metal stable isotope composition between materials tend to be small, a few parts per thousand at most, so that differences in absolute isotope ratio are difficult to conceptualize. For example, say that the $^{53}\text{Cr}/^{52}\text{Cr}$ ratio determined by TIMS for a native groundwater sample is 0.114000, while the value for the Cr isotope standard is 0.113392. To better visualize this small difference, most researchers in the field have adopted the delta notation used for gas isotope ratio comparison so that ratios can be compared on a per mil (‰) basis. Using the Cr example:

$$\begin{aligned} \delta^{53/52}\text{Cr} &= 1000 * \left(\frac{^{53}\text{Cr}}{^{52}\text{Cr}_{\text{groundwater}}} - \frac{^{53}\text{Cr}}{^{52}\text{Cr}_{\text{standard}}} \right) / \frac{^{53}\text{Cr}}{^{52}\text{Cr}_{\text{standard}}} \\ &= 1000 * (0.114000 - 0.113392) / 0.113392 \\ &= +5.36. \end{aligned}$$

δ values are preceded by a plus or minus sign to denote ratios that are, respectively, heavier or lighter

than the reference material, which in this case is NIST 979 Cr metal. There are two important variants of the δ notation: (1) $\Delta_{\text{A-B}}$ may be used to represent the difference in δ values between two samples, A and B; and (2) workers may use the ε notation, equal to 10 times δ , or parts per 10,000, in cases where differences in isotope composition between samples are extremely small. Caution is advised as there are additional uses of both Δ and ε in isotope science terminology, and some researchers report isotope ratio variations on a per atomic mass unit basis.

Standard reference materials (SRM) provide the basis for inter- and intra-laboratory comparison of isotope ratio measurements. While the mass spectrometers used in different laboratories might produce different absolute values for an SRM, the ratios obtained on samples are comparable through use of the delta scale described above, calculated relative to the SRM. Most standards used in metal stable isotope research are supplied by two sources: the Institute for Reference Materials and Measurements (IRMM, Belgium) and the National Institute for Standards and Technology (NIST, USA). Both organizations have gone to great lengths to produce large quantities of metal isotope SRM, which have been rigorously assessed through round-robin analyses at a number of isotope laboratories. A good SRM must (1) be in abundant supply and available for distribution, (2) be homogeneous in isotopic composition across the supply, (3) have an isotopic composition similar to or bordering the range to be measured in samples, and (4) have an agreed-upon value. Ideally, for a given metal it is preferable to have at least two well-characterized SRM that bracket the range of isotope ratios anticipated in samples. This is rarely the case, and thus most researchers rely on a single SRM that is used widely by other laboratories, together with routinely analyzed internal standards used to monitor consistency of laboratory processing and mass spectrometer function. An important point is that all isotope research should be conducted using widely available SRM in order to allow other laboratories to make a check of accuracy.

Commonly used SRM include: Cr, NIST 979; Fe, IRMM-014; Ni, NIST 986; Cu, NIST 976; Zn, JMC (Johnson Matthey Corporation) 3-0749-L and IRMM-3702; Mo, NIST 3134 (proposed; presently there is no internationally accepted SRM (Wen et al. 2010), but acceptance by the isotope community requires a period of inter-laboratory comparison to validate the

choice); Cd, JMC lot 502552A and NIST 3108; Ag, NIST 978a. Note that there are currently no internationally accepted or proposed SRM for Ti, V, W or Re isotope analysis.

IRMM and NIST typically supply an SRM for metal stable isotope analysis in the form of a purified metal or salt, both of which are easy to dissolve and use routinely. However, some researchers choose to use natural samples as standards, provided those samples meet the criteria listed above. The advantage of using a natural material as an SRM is that it must follow the same chemical purification steps as samples, thus assuring integrity of the chemical procedures. For some metals, there are both natural and synthetic SRM. For Fe stable isotope research, for example, there are two widely available SRM: specific basalts and other igneous rocks, which have been shown to have uniform isotope composition (Beard et al. 2003), and IRMM-014, a synthetic iron standard. The isotope composition of IRMM-014 is now generally considered to be the zero point for the delta scale; on this basis, igneous rocks have on average a $\delta^{56/54}\text{Fe}$ value of +0.09‰. Unfortunately, Fe lacks SRM having isotope compositions at the light and heavy extremes of the natural spectrum.

10.3 Metal Stable Isotope Fractionation Processes

Isotope fractionation is a set of processes which can divide an isotopically homogeneous pool of an element into multiple fractions that have different complementary isotope compositions. For a given element, observed fractionation may be either mass dependent, scaling approximately as the mass difference between isotope pairs, or mass independent, where one isotope behaves non-systematically with respect to the others. By far, most of the stable isotope variability of the transition and post-transition metals observed to date has resulted from mass dependent processes.

There are two main categories of isotope fractionation processes that affect the transition and post-transition metals, kinetic isotope effects and equilibrium isotope exchange. Kinetic isotope effects result from uni-directional physical and chemical reactions, during which the light isotope is always

favored in the product phase. Examples of processes resulting in kinetic isotope effects are evaporation, where light isotopes of metals such as Zn and Cd escape more efficiently at the liquid-air interface than heavy isotopes (e.g. Cloquet et al. 2006a, b), electro-plating, where light isotopes of metals from the plating bath are preferentially deposited onto a metal substrate (Kavner et al. 2008), and diffusion (Richter et al. 2009). A special class of kinetic isotope effects arises for elements having differences in specific isotope reaction rates, for example where the odd-numbered isotopes of Hg behave non-systematically with respect to the even-numbered isotopes (Bergquist and Blum 2009; Blum 2011). Isotope equilibrium results from protracted exchange between reaction products and reactants, and at equilibrium the products may be either lighter or heavier than the reactants depending on factors such as metal ion coordination, packing density and bond strength. Examples of processes resulting in isotope equilibrium are the partitioning of relatively heavy Fe into $[\text{Fe(III)}(\text{H}_2\text{O})_6]_{(\text{aq})}^{3+}$ compared to Fe in coexisting $[\text{Fe(II)}(\text{H}_2\text{O})_6]_{(\text{aq})}^{2+}$ (Johnson et al. 2002; Welch et al. 2003), and the exchange of Fe between hematite and $[\text{Fe(III)}(\text{H}_2\text{O})_6]_{(\text{aq})}^{3+}$ leading to identical Fe isotope compositions of these two phases (i.e. no isotope fractionation). This latter example is interesting in that hematite formed initially in synthesis experiments has light Fe relative to coexisting $[\text{Fe(III)}(\text{H}_2\text{O})_6]_{(\text{aq})}^{3+}$ due to kinetic isotope effects that are subsequently reversed (Skulan et al. 2002). Note that isotope equilibrium between liquid and vapor is likewise possible, as in the case of Hg (Estrade et al. 2009). Excellent discussions of the topic of kinetic and equilibrium isotope fractionation, with examples pertinent to environmental studies, are provided by Clark and Fritz (1997) and Kendall and McDonnell (1998).

Redox reactions, whether strictly inorganic or microbially mediated, consistently result in significant metal stable isotope fractionation, and the reduced species of the metal redox pair is generally isotopically lighter than the oxidized species. Thus, determination of the isotope composition of redox-sensitive metals has proven useful for understanding redox dynamics in paleo- and present-day environmental systems (Severmann and Anbar 2009; Bergquist and Blum 2009; Bullen and Walczyk 2009). On the other hand, the stable isotope composition of metals which occur naturally in only one redox state (e.g. Cd, Zn)

but which may fractionate during complexation with redox-sensitive species such as sulfur (Schauble 2003) or with organic matter (Weiss et al. 2007) can likewise be indicative of redox conditions.

Sorption of metals onto the surfaces of minerals in sediments and soils is an environmentally important process that can help to moderate aqueous concentrations of those metals and aid in metal contaminant remediation. Isotope fractionation associated with sorption has been recognized for several of the transition and post-transition metals, but is highly element specific. For example, sorption of isotopically light Mo onto ferromanganese oxides in the oxic oceans is viewed as having been an important isotope fractionation process for Mo over much of Earth history (Wasylenski et al. 2008). In contrast, sorbed Fe(II) on goethite was found to be isotopically heavy compared to $[Fe(II)(H_2O)_6]_{(aq)}^{3+}$ in a series of carefully conducted equilibrium isotope exchange experiments reported by Beard et al. (2010). In the case of Cr, only a negligible isotope fractionation was observed between sorbed and aqueous CrO_4^{2-} and $HCr_2O_7^-$ when either $\gamma-Al_2O_3$ or goethite was used as the sorption substrate (Ellis et al. 2004).

Coordination environment of the metals in liquids and solids is an additional important determinant of stable isotope fractionation. In general, for a given system chemistry, higher coordination favors the lighter isotopes. Using the system Fe-O as an example, Fe in hematite (Fe_2O_3) is in octahedral coordination while Fe in magnetite (Fe_3O_4) is in both octahedral and tetrahedral coordination within their respective oxygen framework. The result is a higher average coordination number for Fe in hematite than for Fe in magnetite. As expected, when the two phases coexist at or near equilibrium, Fe in hematite is isotopically lighter than Fe in magnetite by approximately 3‰, as has been reported for coexisting magnetite-hematite pairs in banded iron formations (Johnson et al. 2003). The difference in metal ion coordination environment in coexisting solid-liquid pairs is likewise an important determinant of stable isotope fractionation. For example, theoretical calculations of equilibrium isotope fractionation predict that aqueous Fe(II), which is in octahedral coordination within a “hexaquo” inner hydration sphere ($[Fe(II)(H_2O)_6]_{(aq)}^{2+}$), should be heavier than Fe(II) in coexisting siderite ($FeCO_3$), in which the Fe(II) is in more open octahedral coordination with oxygen of the carbonate groups (Polyakov

and Mineev 2000; Schable 2004). Siderite synthesis experiments confirm the sense of this theoretical fractionation, but observed magnitudes are less than those predicted by theory (Wiesli et al. 2004). Gaining a better understanding of aqueous metal coordination environments and the implications for stable isotope fractionation is one of the major challenges facing the field.

10.4 Applications of Metal Isotopes to Environmental Studies

The transition and post-transition metals are subject to numerous potential isotope fractionation processes over a wide range of environmental conditions, and thus their isotope compositions may provide a unique record of those processes that can be used to understand present-day and paleo-environmental systems. In this section, several examples are given that illustrate the spectrum of environmental issues that can be addressed using these novel stable isotope tracers as process recorders. These include using the isotopes to trace metal contaminants, to identify metal redox processes, to assess plant nutrition cycles and understand processes within plants, and to serve as biomarkers. Although familiarity with the general topic of stable isotope biogeochemistry will help the reader to appreciate the details of the following examples, the introductory material and references in this and other chapters of this book should help those not familiar with the field to better understand why the isotopes are useful and how they work in these specific cases.

10.4.1 Tracing Metal Contaminant Sources and Sinks

The ability of isotope signatures to trace the sources of and processes affecting metal contaminants in groundwater and the atmosphere appears to be receiving the most attention from research groups focused on environmental applications of transition and post-transition metal stable isotopes. Of metal contaminants in groundwater, Cr(VI) is arguably the best understood in terms of isotope systematics based on laboratory

experiments, and Cr stable isotopes have been used to study the fate of toxic Cr contamination at numerous field sites. Of the potential metal contaminants in the atmosphere, the most progress has been made in understanding Hg sources and sinks as discussed by Blum (2011), but Zn, Cd and Cr are likewise receiving considerable attention and are discussed here.

10.4.1.1 Tracing Sources of Chromium in Groundwater

As described above in the overview of Cr, reduction of Cr(VI) to Cr(III) is accompanied by a large isotope fractionation. Thus, Cr stable isotopes should be useful for monitoring Cr(VI) reduction in a contaminant plume, for distinguishing between Cr(VI) reduction and advective mixing with Cr-free groundwater (two mechanisms that can decrease Cr(VI) concentrations in the contaminant plume), and potentially for distinguishing between industrial and natural sources of Cr (VI). Sources of Cr used for industrial purposes are likely to be Cr ore deposits and minerals, which consistently have $\delta^{53/52}\text{Cr}$ values close to 0‰ relative to NIST 979 (Ellis et al. 2002; Schoenberg et al. 2008). In contrast, naturally occurring Cr in groundwater displays a range of values ($\delta^{53/52}\text{Cr}$: +1.0 to +5.8‰; Ellis et al. 2002; Izbicki et al. 2008). These values likely reflect fractionation during oxidation of Cr(III) on manganese oxides and fractionation during subsequent reduction of Cr(VI) along groundwater flowpaths following mobilization of the highly soluble Cr(VI) from mineral surface sorption sites. Thus under favorable conditions the natural and industrial Cr pools at a contaminated site may have different $\delta^{53/52}\text{Cr}$ values.

In order to test the usefulness of Cr stable isotopes for Cr contamination source assessment and process identification at a well-studied contaminated site, a pilot study (CH2MHill 2007) was carried out at the Pacific Gas & Electric (PG&E) Compressor Facility in Hinkley, California, made famous in the movie “Erin Brockovich.” From 1952 to 1966, waste water containing Cr(VI) used as an anti-corrosive in the cooling towers leaked into the underlying sandy aquifer, creating a plume of Cr(VI)-contaminated groundwater that by 2000 had migrated nearly 2 miles downgradient from the facility. Groundwater samples from immediately adjacent to the facility, from within the plume, and of regional groundwater

collected well away from the plume were analyzed for Cr stable isotope composition (Bullen 2007). As shown in Fig. 10.3, the data plot along a well-organized trend, with near-facility (contaminant) and regional groundwaters defining the extremes, while samples from the contaminant plume plot in between. There is no question that in this particular case, the Cr stable isotopes clearly distinguish the natural and anthropogenic Cr(VI) end-members.

It is less clear how the samples collected from the contaminant plume obtained their compositions in $\delta^{53/52}\text{Cr}$ -Cr concentration space. For example, as shown in Fig. 10.3 the plume sample data all lie well to the low-Cr side of model trends describing both abiotic and microbially-mediated Cr(VI) reduction (Ellis et al. 2002; Sikora et al. 2008) and well to the high- $\delta^{53/52}\text{Cr}$ side of the model trend for advective mixing between near-facility contaminant and regional groundwaters, suggesting that neither Cr(VI) reduction nor advective mixing alone is able to account for those compositions. However, some combination of Cr(VI) reduction and advective mixing could account for the plume sample compositions, and a scenario that is at least consistent with field relations (Bullen 2007) is shown in Fig. 10.3. In this scenario, Cr(VI) at the front and margins of the migrating contaminant plume would come into contact with the limited reductant (e.g. ferrous iron, organic matter) in this aquifer, allowing small amounts of Cr(VI) reduction to occur and driving remnant Cr(VI) compositions along the model Cr(VI) reduction vectors. At the same time, advective mixing with regional groundwaters at the plume front and margins would shift remnant Cr(VI) compositions to the low-Cr side of the model Cr(VI) reduction vectors (e.g. along trajectories similar to the lines labeled “plume front Cr(VI) reduction-mixing” in Fig. 10.3). After 40 years of plume migration, one could imagine an array of developed plume front and margin groundwater compositions similar to region “FM” in Fig. 10.3. This range of plume front and margin groundwater compositions would result from specific evolutionary trends that depend on the relative amount of Cr(VI) reduction and advective mixing with regional groundwater that occurred at any particular position along the plume front or margin. In this scenario, the actual plume sample array would develop by advective mixing between these hypothesized plume front and margin groundwaters and the contaminated groundwater

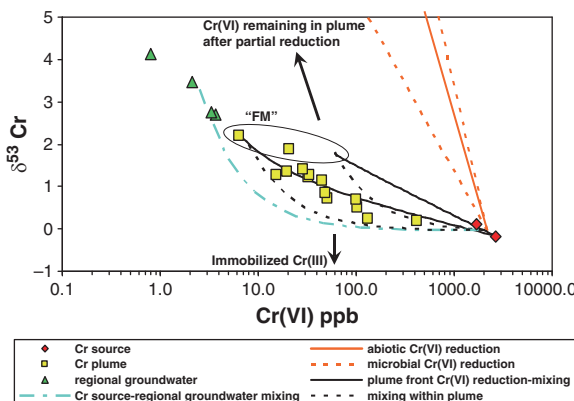


Fig. 10.3 $\delta^{53/52}\text{Cr}$ and Cr(VI) concentration data for groundwater at the Hinkley, CA site “Cr source” samples were collected at the PG&E compressor facility, “Cr plume” samples were collected downgradient of the compressor facility within the Cr(VI) plume. “Regional groundwater” samples were collected just upgradient, just down gradient, and well away from the plume. The “Cr source-regional groundwater mixing” curve shows mixing between Cr source and average regional groundwater. The “abiotic Cr(VI) reduction vector” is from Ellis et al. (2002); the “microbial Cr(VI) reduction” vectors are from Sikora et al. (2008), and show the range of fractionation observed in their experiments. The field labeled “FM” represents plume Front and Margin samples produced through combined Cr(VI) reduction and advective mixing with regional groundwater as described in the text. The “mixing within plume” curves show mixing between “FM”-type and “Cr source” groundwaters. The arrow labeled “Cr(VI) remaining in plume following partial reduction” shows the direction that homogeneous Cr(VI) reduction within the plume will move residual Cr(VI) compositions on this diagram. The arrow labeled “immobilized Cr(III)” shows that Cr(III) produced during Cr(VI) reduction will have negative $\delta^{53/52}\text{Cr}$. The uncertainty of the data for all samples is less than the size of the symbol

within the plume body itself. Note that extremely careful, discrete depth sampling at the plume front and margins would be necessary to confirm the existence and determine the exact shape of the “FM” region hypothesized in Fig. 10.3, but such an effort would be useful for supporting the validity of this proposed scenario.

In their detailed time-series study of a point-source Cr contamination plume emanating from a Cr plating facility in Berkeley, California, Berna et al. (2010) observed a similar trend for plume groundwater samples in $\delta^{53/52}\text{Cr}$ -Cr concentration space, such that the plume samples had intermediate compositions between vectors describing Cr(VI) reduction and advective mixing with Cr-free groundwater. Although

they concluded that Cr(VI) reduction and advective mixing were important processes determining the composition of the plume groundwater samples, they likewise pointed to the potential importance of heterogeneous Cr(VI) reduction in the aquifer. Their laboratory incubation experiments had demonstrated that Cr (VI) reduction was limited to greenish, fine-grained lenses that are embedded in non-reducing aquifer materials. They proposed that total reduction of small pools of Cr(VI) in the greenish lenses would decrease the amount of Cr(VI) measured in a down-gradient sampling well, but would not change the $\delta^{53/52}\text{Cr}$ value of the remaining Cr(VI) transported through the non-reducing aquifer materials. As a result, the $\delta^{53/52}\text{Cr}$ value of groundwater sampled along the plume is not as high and the $\delta^{53/52}\text{Cr}$ value of Cr(III) immobilized on the aquifer sediment is not as low as would be predicted for a system where reduction occurs homogeneously throughout the aquifer. As at Hinkley, careful discrete depth sampling would help to determine the influence of aquifer heterogeneity on Cr(VI) reduction effectiveness and measured $\delta^{53/52}\text{Cr}$ values.

10.4.1.2 Sources of Zinc in River Water

As described above in the overview on Zn, there are several processes that may result in Zn stable isotope fractionation including biological incorporation, abiotic adsorption, chemical diffusion and industrial processing. Although Zn is not a highly toxic metal it does provide a useful index of environmental contamination because it is commonly associated with toxic metals such as Cd and Pb. Thus Zn stable isotopes may be useful for distinguishing natural and anthropogenic sources of metals in both hydrologic and atmospheric systems.

An interesting example of the usefulness of Zn isotopes to trace contaminant sources is the work of Chen et al. (2008, 2009) who studied Zn isotope systematics of the Seine River of France. The Seine River is one of the most anthropogenically impacted rivers in Europe, with high relative concentrations of metals (Zn, Cu, Pb, Ni, etc.) in dissolved and suspended loads compared to large rivers of the world (Chen et al. 2009). For their study, these workers sampled both the dissolved and suspended particulate matter (SPM) fractions of Seine River waters along the length

of the river and, during both high and low flow periods, in the center of the city of Paris. This sampling strategy allowed these workers to test for a Zn isotope signal of industrial and urban activity, since most industry is concentrated in and downstream of Paris.

Chen et al. (2009) observed an overall negative correlation between $\delta^{66/64}\text{Zn}$ of SPM and the Zn enrichment factor (EF), which describes the enrichment of Zn in a sample relative to the natural background and is defined as:

$$\text{EF} = (\text{Zn}/\text{Al})_{\text{sample}} / (\text{Zn}/\text{Al})_{\text{background}}$$

where $(\text{Zn}/\text{Al})_{\text{background}}$ was estimated using average concentrations of Zn and Al in uncontaminated forest sediments and pre-historical deposits as assessed by Thevenot et al. (2007). Specifically, as shown in Fig. 10.4a, SPM samples with lesser $\delta^{66/64}\text{Zn}$ and greater Zn EF were those collected within Paris during the low flow periods and from downstream of Paris. Chen et al. (2009) identified two potential anthropogenic contaminant sources, Zn in roof runoff from buildings in Paris and waste water treatment plant effluent, each having low $\delta^{66/64}\text{Zn}$ and high Zn EF that could explain the low flow Zn isotope signal. In contrast, background Zn from upstream sources was determined to have elevated $\delta^{66/64}\text{Zn}$ and low Zn EF based on analyses of bedrock from the region (the composition for bedrock granite from the region is shown in Fig. 10.4a) and the compositions of SPM from upstream of Paris.

Chen et al. (2009) observed additional complexity when they considered $\delta^{66/64}\text{Zn}$ of SPM and $\delta^{66/64}\text{Zn}$ of dissolved Zn together (Fig. 10.4b). Seine Basin transect and Paris low flow samples defined a linear array that could be explained by mixing between natural and anthropogenic end-members. The natural end-member (Zn_{nat}) was inferred to have $\delta^{66/64}\text{Zn}$ of SPM similar to that of bedrock granite (+0.33‰) and $\delta^{66/64}\text{Zn}$ of dissolved Zn similar to that of Cretaceous chalk from the region (+0.90‰), highlighting the fact that Zn in SPM and the dissolved phase can come from different sources. Some Paris high flow samples required an additional component, again having $\delta^{66/64}\text{Zn}$ of SPM similar to that of bedrock granite, but having $\delta^{66/64}\text{Zn}$ of dissolved Zn reflecting a mix-

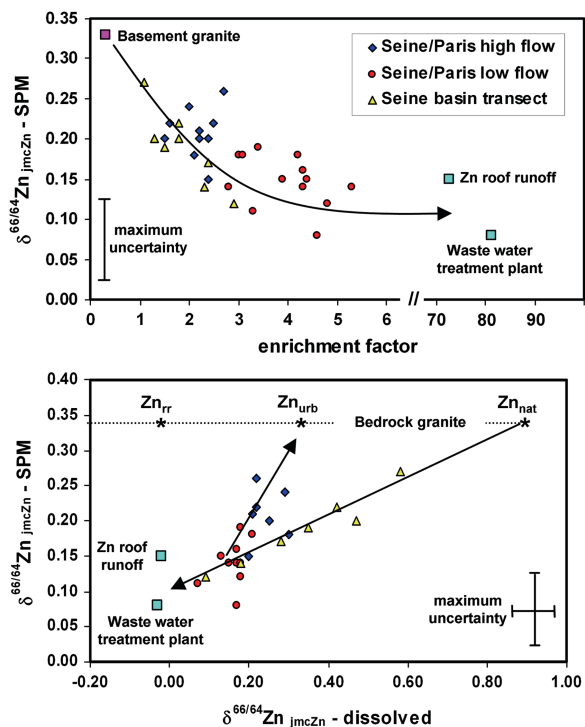


Fig. 10.4 Zn isotope systematics of the Seine River, modified after Chen et al. (2008, 2009). (a) $\delta^{66/64}\text{Zn}$ of suspended particulate matter (SPM) vs. the Zn enrichment factor (defined in text). Curved vector describes mixing between a natural end-member, basement granite, and likely anthropogenic end-members, Zn roof runoff and waste water treatment plant effluent. Note break in enrichment factor scale. (b) $\delta^{66/64}\text{Zn}$ of SPM vs. $\delta^{66/64}\text{Zn}$ of dissolved Zn. Symbols are the same as in Fig. 10.4a. Zn isotope compositions of basin transect and Paris low flow samples can be explained as mixtures of a natural end-member (Zn_{nat} , having $\delta^{66/64}\text{Zn}$ of SPM dominated by bedrock granite and $\delta^{66/64}\text{Zn}$ of dissolved Zn dominated by Cretaceous chalk), and an anthropogenic end-member having Zn isotope composition similar to that of Zn roof runoff and waste water treatment plant effluent. Paris high flow samples require an additional “urban” end-member (Zn_{urb} , having $\delta^{66/64}\text{Zn}$ of SPM dominated by bedrock granite and $\delta^{66/64}\text{Zn}$ of dissolved Zn reflecting a mixture of Cretaceous chalk Zn and Zn from roof runoff (Zn_{rr}). Errors are equal to or less than maximum uncertainty bars shown

ture of Zn from Cretaceous chalk (the dissolved component of Zn_{nat}) and the dissolved component of Zn from roof runoff (Zn_{rr}). Chen et al. (2009) suggested that urban Zn storm runoff (Zn_{urb}) adds considerable dissolved Zn but only minor SPM associated with zinc roofing materials to the river.

10.4.1.3 Tracing Sources of Metals in Dust Using a Multi-Tracer Approach

Inhalation of dust particles is potentially a primary delivery mechanism of toxic metals to humans. Moreover, incorporation of deposited dust in soil can allow the metals to become available to plants, providing an additional source of metal loading to crops. There are many possible sources of transition and post-transition metals that could supply the metal content of dust. The major contributors are likely to include metal refining and smelting, coal combustion fly ash and residues, petroleum burning and particularly vehicle emissions, municipal waste incineration, scrap metal deterioration, and wood burning. Early approaches for identifying dust sources relied on tracers such as concentration ratios of metals and surrogates such as strontium isotopes that might be able to tie the dust back to specific geologic or regional sources. While there have been numerous examples of success with this approach, environmental isotope scientists have been exploring whether the stable isotope composition of the transition and post-transition metals might be more directly useful for fingerprinting the sources of the metals in dust.

Of the potential sources for these metals listed above, metal refining and smelting have received the most attention, mainly for Zn and Cd, pointing to the unique physical characteristics of these two post-transition metals. As noted above in the overview on these elements, their boiling points are sufficiently low that they can both be evaporated in the smelter furnace, resulting in a kinetic isotope fractionation that partitions light metal into the vapor that escapes the factory stack. For Zn, light compositions in refinery stack emissions have been documented by Mattielli et al. (2009), while heavy compositions in residual slag compositions have been documented by Sivry et al. (2009). For Cd, the same sense of isotope fractionation was observed for smelter exhaust and slag by Cloquet et al. (2006a). Mercury similarly has a low boiling point within the range of smelter and waste incinerator furnace temperatures, and partitioning of light Hg into stack emissions has been proposed (Estrade et al. 2010). Thus the association of light Zn, Cd, and Hg, along with unfractionated compositions relative to the ore sources for other metals having far greater boiling points (such as Cr and Cu) could implicate a metal refining smelter exhaust stack source for those metals in dust samples.

The Zn and Cd stable isotope compositions of the other potential sources of metals in dust listed above are less constrained, although some reconnaissance values for Zn are available in the literature. Cloquet et al. (2006b) reported $\delta^{66/64}\text{Zn}$ values for particulates trapped on bus air filters and emitted in urban waste incinerator flue gas from Metz, France, which spanned a small range from +0.04 to +0.19‰ relative to the JMC-Lyon Zn standard. On the other hand, lichens collected from around Metz that had high Pb concentrations and Pb isotope signatures consistent with a leaded gasoline source likewise had high Zn concentrations and negative $\delta^{66/64}\text{Zn}$ (to -0.2‰), suggesting that light Zn might be associated with road traffic circulation. Sivry et al. (2008) reported $\delta^{66/64}\text{Zn}$ of +0.72‰ for a coal ash from southwest France, which is consistent with the association of heavy Zn with organic materials recognized by Weiss et al. (2007).

In their study of sources of metals observed in dust samples collected in Paris, France, Widory et al. (2010) have expanded this emerging isotope database for the sources and specifically have measured Zn, Cd, and Cr stable isotope compositions for each of their samples. Important aspects of their data, shown in Fig. 10.5a and b, include: (1) a broad range of $\delta^{114/110}\text{Cd}$ for particulates in vehicle exhaust; (2) the tendency of organic-associated materials such as fuel oil and coal to have positive $\delta^{66/64}\text{Zn}$; and (3) the positive $\delta^{53/52}\text{Cr}$ values of the coal combustion samples, perhaps reflecting the particular redox history of the coal deposit. These data highlight the potential variability of the anthropogenic signal and show the utility of the multi-isotope approach.

Although the influence of dust from deteriorating metal in scrapyards has yet to be rigorously quantified in terms of either metal flux or stable isotope composition, there is potentially an important isotope signal resulting from electroplating as noted above. Electroplating is a ubiquitous process that can produce an isotopically light pool for all the transition and post-transition metals (e.g. Kavner et al. 2008), and recognition of light isotope compositions for a suite of metals such as Zn, Cd and Cr in a set of dust samples may point to such sources. Cadmium and Zn isotope compositions of an electroplated metal nut and Cr and Zn isotope compositions of an electroplated metal bolt, measured by the author, are included in Fig. 10.5a and b to illustrate the potential signal.

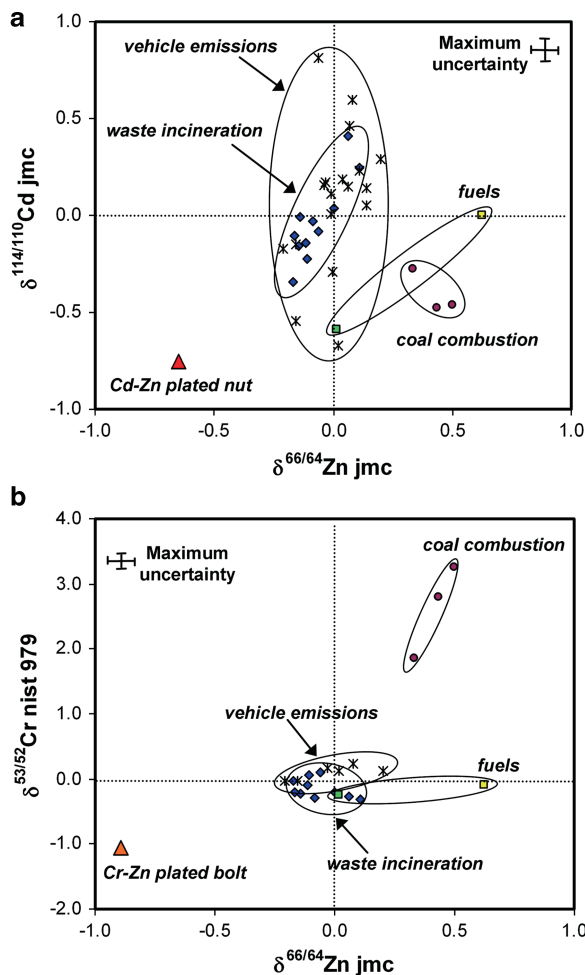


Fig. 10.5 (a) Cd-Zn and (b) Cr-Zn isotope systematics of suspected sources of metals in dust from northern France. Measurements were made on acid leachates of particles collected at municipal waste incinerators and coal combustion plants, from vehicle exhaust pipe filters, on acid leachates of plated nuts and bolts, and on total digests of fuels. Modified from Widory et al. (2010) with additional unpublished data from author

The obvious need to understand the potential influence of deteriorating electroplated metal stockpiles on the isotope composition of atmospheric dust, perhaps mostly to monitor the global transport of potentially toxic metals, makes this an important avenue for future research.

10.4.2 Metal Redox Cycles

The common association of changes in redox status of the transition and post-transition metals with isotope

fractionation between oxidized and reduced states points to the potentially powerful application of the isotopes as tracers of redox cycles in natural systems. Isotopes can be used, for example, to distinguish between biological and geochemical processes, such as microbial reduction and inorganic oxidation, and physical processes, such as advective mixing and diffusion, to explain chemical and isotopic composition gradients in hydrologic systems.

Teutsch et al. (2009) used Fe isotopes to study the Fe cycle across the oxic-anoxic boundary of meromictic Lake Nyos, Cameroon, the site of a sudden catastrophic release of CO₂ in 1986 that killed about 1,700 people. To avoid the recurrence of catastrophic outgassing of CO₂ that is supplied by groundwater to the lake bottom, the lake is now artificially degassed by a tube that drains deep water to the surface (Kling et al. 2005). The degassing system spreads deep water with concentrations of dissolved Fe(II) in a high jet over the lake, causing immediate oxidation of the Fe (II) to Fe(III)-oxyhydroxide particulate which then settles into the lake. Concentrations of dissolved Fe(II) in the oxic surface waters are negligible, but sharply increase as particles settle across the oxic-anoxic boundary at depth. Partial reduction of the Fe(III)-rich particles at this boundary releases Fe(II) to solution, which then diffuses upwards into the oxic zone where it is re-oxidized to form Fe(III)-oxyhydroxides which settle back to the oxic-anoxic boundary, and the cycle continues.

Depth profiles sampled in the lake revealed a sharp increase in both dissolved Fe(II) concentrations and $\delta^{57/54}\text{Fe}$ values in a thin zone across the oxic-anoxic boundary. Using a calibrated one dimensional reaction-transport model that considered the isotopic signatures of dissolved Fe(II) and the settling of Fe (III)-rich particles, the settling fluxes of the particles and the dissolved Fe(II) concentration profiles, Teutsch et al. (2009) showed that the sharp increase in $\delta^{57/54}\text{Fe}$ values is caused by isotopic fractionation associated with dissimilatory Fe(III) reduction across the oxic-anoxic boundary. They further showed that the continued shift toward even greater $\delta^{57/54}\text{Fe}$ values below the oxic-anoxic boundary is due to vertical mixing of Fe-rich lake bottom water that has high- $\delta^{57/54}\text{Fe}$ values, perhaps due to precipitation of siderite. In this study, isotopic analyses coupled to modeling proved invaluable for identifying the

processes responsible for the broad range of $\delta^{57/54}\text{Fe}$ values observed in this lake.

Isotopes can likewise be used to assess paleoredox conditions in water bodies, for example by looking at variations of the redox-sensitive Mo isotope composition of sediments. In oxic settings, Mo isotopes are fractionated during adsorption of Mo to ferromanganese oxides, with light isotopes preferentially associated with the solids. Experimental work under oxidizing conditions has shown that $\delta^{97/95}\text{Mo}$ of aqueous Mo in seawater is 2.7‰ greater than that of adsorbed Mo on sediment (Barling et al. 2001; Barling and Anbar 2004; Wasylewski et al. 2008). As waters progress from oxic to suboxic to anoxic to euxinic (i.e. sulfidic) conditions, MoO_4^{2-} is converted to MoS_4^{2-} which readily adsorbs to particles allowing aqueous Mo to be more effectively removed to the sediment (Poulson et al. 2006; Neubert et al. 2008). The net result is that the isotopic contrast between aqueous and sorbed Mo is greatest at slightly reducing conditions and low sedimentation rates, but decreases with increasingly reducing and sulfidic conditions due to increasingly more quantitative removal of Mo from solution.

This concept was used by Siebert et al. (2006) to account for differences in the average Mo isotope composition of sediment profiles from continental margin settings. These workers recognized a co-variation between the Mo isotope composition of the sediments and the rate of both authigenic Mo accumulation and organic carbon oxidation and burial under reducing conditions. Malinovsky et al. (2007) tried the same approach to understand paleoredox cycles in lakes from northern Sweden and northwestern Russia, where variations of Mo isotope composition in the sediments could be attributed to both redox status of the water column and isotopically variable input of Mo into the lakes due to Mo isotopic heterogeneity of bedrock in the drainage basins. This latter study points to the need for rigorous source term characterization, particularly as study site size decreases from global to local scale.

An area of applied research where transition and post-transition metal stable isotopes are increasingly being used is to understand sedimentary and low temperature hydrothermal metal redox cycling, where both inorganic and biological redox processes can cause isotope fractionation. For example, Asael et al. (2007) used Cu stable isotopes to understand Cu redox cycling and mass transfer functions during sequential

cycles of low temperature alteration of igneous copper porphyries, marine sedimentary diagenesis and epigenetic mobilization of Cu in sandstones at a site of historic Cu mining in southern Israel. As predicted by theory and experiment, they found that $\delta^{65/63}\text{Cu}$ values of Cu(I)-sulfides in the stratiform sediment-hosted Cu deposits are significantly lower than those of coexisting Cu(II)-carbonates and hydroxides. Coupling the Cu isotope composition of the minerals to a mass balance model revealed that the main Cu reservoir of the ore body is a sandstone-shale sequence and that the importance of Cu-sulfide reservoirs is small, consistent with field observations. Thus most of the Cu transport occurred in relatively oxidized conditions, the knowledge of which provides a novel tool for exploration in the future.

10.4.3 Plant Nutrition and Processes Within Plants

Numerous transition and post-transition metals play important chemical roles in plant nutrition (Marschner 1995). For example, of the metals discussed in this chapter, Fe is essential for chlorophyll development and function, assists in energy transfer functions and redox reactions, is an important constituent of enzymes and participates in nitrogen fixation. Zinc is important for carbohydrate and protein metabolism, pollen formation, and general disease resistance, and is a structural constituent or regulatory co-factor of numerous plant enzymes. Molybdenum, Cu and Ni each play additional important physiological roles in plant nutrition, while excesses can lead to a variety of toxic effects on plant vitality. Using the stable isotopes of these metals as indicators of metal sources and cycling processes, and perhaps to reveal the onset of metal toxicity, is an emerging field in isotope biogeoscience.

As pointed out by von Blanckenburg et al. (2009), the metabolic processes that control the behavior of metals in plants can be envisaged as a gigantic geochemical pump that continuously moves metals between reservoirs. As plants move metals from soils into roots and along the transpiration stream, the metals are cycled through a variety of chemical species via processes that can lead to isotope

fractionation. During the past several years, for the metals discussed here stable isotope fractionation in higher plants has been demonstrated for Fe and Zn (Weiss et al. 2005; Guelke and von Blanckenburg 2007; Viers et al. 2007; Moynier et al. 2008; Kiczka et al. 2010). This is an intriguing pair of metals to consider, as the isotope fractionations observed in plants are largely controlled by redox status for Fe, and by complexation chemistry for Zn.

Plants have developed two different strategies for transporting Fe from soils into roots. Roots of dicotyledons and nongraminaceous monocotyledons (“strategy I plants”, e.g. pea, bean) release protons into the rhizosphere, promoting dissolution of Fe(III) precipitates, and activating membrane-bound enzymes that reduce chelate-bound Fe(III). The reduced Fe is then transported across the root plasma membrane by unspecific metal transporters (Briat et al. 2007). Partial reduction of an Fe(III)-solid produces aqueous Fe(II) with an $\delta^{56}\text{Fe}/\delta^{54}\text{Fe}$ ratio that is approximately 1–1.5% less than that in the remaining Fe(III)-solid (Johnson et al. 2004). As a consequence, the Fe(II) that crosses the root plasma membrane, and thus the pool of Fe in a strategy I plant, is lighter than the soil Fe pool. In contrast, roots of graminaceous plant species (“strategy II plants”, e.g. maize, wheat) can release phytosiderophores into the rhizosphere, which form complexes with Fe(III) (Romheld and Marschner 1986; Kraemer et al. 2006). These Fe(III)-complexes are then transported across the root plasma membrane by a specialized class of transport proteins, but due to

lack of reduction, the pool of Fe(III) in a strategy II plant has the same Fe isotope composition as the soil Fe pool.

The results of two studies of Fe isotope variability in plants are shown in Fig. 10.6. In a variety of strategy I plants studied by Guelke and von Blanckenburg (2007), $\delta^{56}\text{Fe}$ values of tissues decreased from soils to stems, from stems to leaves and from leaves to seeds. In contrast, all tissues in their strategy II plants had similar $\delta^{56}\text{Fe}$ values, which they attributed to differences in the way that Fe is translocated in the two plant types. These results are consistent with the different Fe uptake and transport processes proposed above for strategy I and strategy II plants. Kiczka et al. (2010), working with strategy I and II plants collected from a recently deglaciated site, identified several reaction points along the translocation stream of both plant types where Fe(III) reduction and thus isotope fractionation might occur, including between the root symplast and apoplasm, between the leaf cytoplasm and the xylem, and between the phloem and the leaf cytoplasm, at each step moving lighter Fe along the transpiration stream. However, in contrast to the results of Guelke and von Blanckenburg (2007), Kiczka et al. (2010) observed similar Fe isotope patterns in their strategy I and II plants, with $\delta^{56}\text{Fe}$ values generally increasing from root stele to stem to leaf. To explain this discrepancy, they pointed to previous studies suggesting that release of siderophores by strategy II plants into the rhizosphere is suppressed under Fe-rich soil conditions similar to

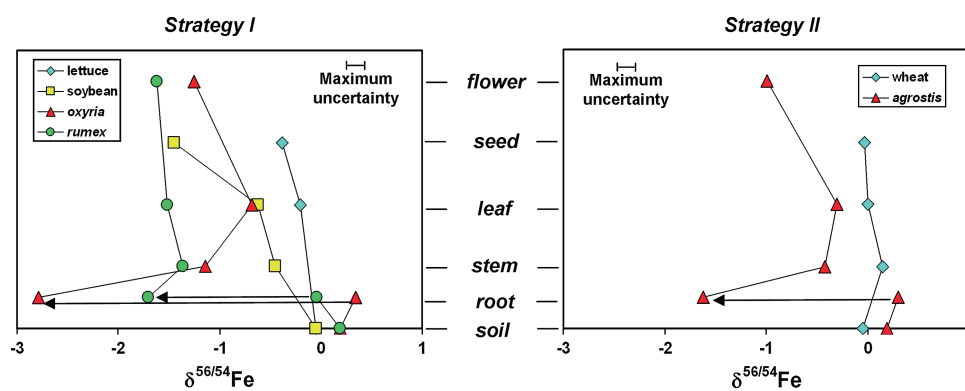


Fig. 10.6 $\delta^{56}\text{Fe}/\delta^{54}\text{Fe}$ values for a variety of plant tissues. Values for lettuce and soybean (Strategy I) and wheat (Strategy II) are from Guelke and von Blanckenburg (2007), values for *oxyria digyna* and *rumex scutatus* (Strategy I) and *agrostis givantea* (Strategy II) are from Kiczka et al. (2010). In each diagram, the arrows between root tissues point from cortex to stele, and

demonstrate the large Fe isotope fractionation that occurs across the plasma membrane. Complex Fe isotope variations within individual plants result from a variety of possible isotope fractionation processes which can occur along the transpiration stream

those at their field site (Marschner 1995), and suggesting that strategy I and II plants mobilize and transport Fe similarly under such conditions (Charlson and Shoemaker 2006).

In the case of Zn, dissolution of Fe(III) solids in the soil by protons released from plant roots results in release of Zn that is adsorbed on the Fe(III) solids. Subsequent uptake of Zn by roots depends only on the induction of specific Zn transporters, which belong to the same protein family as the Fe transporters (Kramer et al. 2007). Likewise, the release of phytosiderophores benefits the acquisition of Zn (Suzuki et al. 2006). Apparently the transport of Fe and Zn to plant roots is closely linked. Zn isotope variability within plants appears to be fairly straightforward and similar for strategy I and strategy II plants, based on several laboratory and field based studies (Weiss et al. 2005; Viers et al. 2007; Moynier et al. 2008). Roots tend have the heaviest Zn, probably reflecting the preferential adsorption of heavy Zn onto the root and plaque surfaces. However it should be noted that the possibility of Zn isotope contrast between the root cortex and stele of plants has yet to be explored, as has been done for Fe isotopes (Kiczka et al. 2010). Shoots have similar to lesser $\delta^{66/64}\text{Zn}$ values than bulk roots, and leaves invariably contain the lightest Zn in the plants. These observations are consistent with light Zn isotopes being transported preferentially during nutrient exchange along the cell walls of the xylem although it is unclear at this stage whether this is a kinetic or an equilibrium process (von Blanckenburg et al. 2009).

There clearly remains much to be done to understand the causes of transition and post-transition metal stable isotope fractionation in plants, and certainly the remaining metals deserve at least a thorough reconnaissance for a variety of plant species and field situations. To date, much of the work has aimed at explaining observed variations of isotope composition in terms of known plant processes. With greater understanding, future work will gradually shift toward using the isotopes to identify as yet unknown or unconstrained processes in plants.

10.4.4 Biosignatures

One of the most enduring hopes and goals of metal stable isotope biogeochemistry is to be able to use the isotopes as biosignatures, by developing either single

or multi-tracer tests that could be applied to a natural system to decipher a biological influence on its origins. A recurring theme in metal stable isotope studies of biological systems is that biological activities that result in significant isotope fractionation generally involve preferential processing of lighter isotopes from the metal source pool into and within the biological materials (e.g. Zhu et al. 2002; Bermin et al. 2006; Johnson et al. 2008; Eisenhauer et al. 2009). Indeed, in the early days of the transition and post-transition metal stable isotope data explosion (i.e. the late 1990s), the general thinking was that most metal stable isotope fractionation observed in nature would be due to biological processing (e.g. Beard and Johnson 1999). This thinking led to pioneering attempts to constrain experimentally an Fe isotope biosignature (Beard et al. 1999), but likewise inspired early attempts to demonstrate the importance of inorganic processes that could fractionate Fe isotopes both in the laboratory (e.g. Anbar et al. 2000) and in natural settings (e.g. Bullen et al. 2001). We now realize that ranges of metal stable isotope fractionation caused by inorganic processes can exceed and overlap those produced by biological processing, making development of robust metal stable isotope biosignature tools a challenge but also an exceptional research opportunity.

Given the early and persistent focus on the isotope systematics of Fe, it is not surprising that the greatest progress toward development of a metal stable isotope biosignature has been for Fe, at least for early Earth environments. As stressed by Johnson et al. (2008), the fluxes of mobilized Fe must have been far greater in the Archean and early Proterozoic because of the enormous amount of Fe-rich sediments (e.g. banded iron formations) that were deposited in that time span. The Fe isotope composition of those sediments is highly variable compared to igneous rocks, implying that the processes responsible for fractionating Fe must have been especially active and variable in extent during that time span. Because microbial dissimilatory Fe reduction (DIR) appears to be the most important process capable of producing large quantities of isotopically light Fe, by an order of magnitude or more compared to inorganic processes, DIR is likely to have been the dominant process affecting Fe during that time span.

In this case, the effectiveness of the Fe isotope biosignature depended on knowledge of the relative sizes of the reduced and oxidized Fe pools during early

Earth history. If we are going to be able to use Fe isotopes to detect a record of DIR in other environments (e.g. in the search for life on Mars and other planetary bodies), we must be able to assess the size of those pools in those environments as well. Confidence in the approach will increase as more terrestrial field sites are studied. A promising example from modern Earth comes from the work of Severmann et al. (2008), who used Fe isotopes to support their contention that DIR coupled to Fe(II) oxidation in oxic shelf sediments can account for the large amount of isotopically light Fe produced on the shelf and shuttled to the euxinic basin of the Black Sea.

Biosignatures based on the other transition and post-transition metal isotope systems have yet to be explored as deeply as that based on Fe, but there are promising signs for success. For example, Borrok et al. (2008) documented a diel cycle for dissolved Zn concentrations and $\delta^{66/64}\text{Zn}$ values in Prickly Pear Creek, which drains a former mining district in the Boulder Batholith, Montana, USA. They found that dissolved Zn concentrations and $\delta^{66/64}\text{Zn}$ values were inversely correlated, with Zn at low concentrations in the daytime having elevated $\delta^{66/64}\text{Zn}$ due to sequestration of light Zn in bed sediments. Biological uptake of light Zn was invoked to explain this relationship, since adsorption of Zn onto amorphous Fe(III) oxides prevalent in bed sediments preferentially concentrates heavy Zn onto sorption sites (Balistrieri et al. 2008). As discussed above, Cameron et al. (2009) demonstrated that methanogenic bacteria cultured in the laboratory preferentially assimilate and retain isotopically light Ni, while a wide range of geologic materials have uniform Ni isotope composition. Nickel isotopes are thus likely to become an important biosignature of methanogenesis. And, as pointed out by von Blanckenburg et al. (2009), plant tissues recycled into soil generally have different metal stable isotope composition than the growth medium, thus the upper soil may retain a time-integrated metal isotope fingerprint of plant activity. New biosignatures are likely to emerge as well understood biological systems are studied.

materials. Arguably, much of the work that has been done to date with the transition and post-transition metal stable isotopes has resulted in a better understanding of the isotope systems themselves rather than the materials that have been measured. Many observed variations in isotope composition have been explained in terms of well understood physical, chemical and biological processes, but isotope analyses have so far rarely revealed some unanticipated or poorly understood set of processes. On the other hand, useful applications pertinent to environmental studies are beginning to emerge: isotopic characteristics of plant homeostasis are being established, multi-tracer approaches for identifying metal sources are being developed, biosignatures are being rigorously constrained through analysis of well understood geological and biological materials, and the isotopic signatures of redox reactions are being characterized. As understanding of metal stable isotope systematics increases, it will become easier to think of novel ways that isotopes can enhance understanding of complex processes in environmental systems.

What should be clear from this chapter is that the field of transition and post-transition metal stable isotope biogeochemistry is really just beginning to mature, and that opportunities are abundant. Major advances over the next several years are likely to include: improving the routine precision and reproducibility of total procedural replicate measurements of samples to the few hundredths of a per mil level; developing robust multi-tracer approaches to identify metal sources and pathways for forensic purposes; looking for the unexpected isotope fractionation of metals such as Ti and Ni in environmental systems; expanding the list of robust biosignatures, including the fingerprint of anthropogenic activities; exploring the metal stable isotope signals of global climate change. This is only a partial list, but one where success is likely to be realized through well-crafted interdisciplinary efforts, careful selection of field sites, and clever laboratory- and field-based experiments.

10.5 Future Directions

As pointed out by Severmann and Anbar (2009), the field of metal stable isotope biogeochemistry emerged primarily as an analytical pursuit driven by advances in mass spectrometry applied to interesting geological

References

- Albarède F, Beard B (2004) Analytical methods for non-traditional isotopes. In: Johnson CM, Beard BL, Albarède F (eds) *Geochemistry of non-traditional stable isotopes*.

- Reviews of Mineralogy and Geochemistry, vol 55. Mineralogical Society of America, Washington, pp 113–152
- Anbar AD (2004) Molybdenum stable isotopes: observations, interpretations and directions. *Rev Mineral Geochem* 55: 425–454
- Anbar AD, Roe JE, Barling J, Nealson KH (2000) Nonbiological fractionation of iron isotopes. *Science* 288:126–128
- Anbar AD, Jarzecki AA, Spiro TG (2005) Theoretical investigation of iron isotope fractionation between $\text{Fe}(\text{H}_2\text{O})_6^{3+}$ and $\text{Fe}(\text{H}_2\text{O})_6^{2+}$: implications for iron stable isotope geochemistry. *Geochim Cosmochim Acta* 69:825–837
- Arnold GL, Anbar AD, Barling J, Lyons TW (2004) Molybdenum isotope evidence for widespread anoxia in mid-Proterozoic oceans. *Science* 304:87–90
- Asael D, Matthews Bar-Matthews M, Halicz L (2007) Copper isotope fractionation in sedimentary copper mineralization (Timna Valley, Israel). *Chem Geol* 243:238–254
- Balci N, Bullen TD, Witte-Lien K, Shanks WC, Motelica M, Mandernack KW (2006) Iron isotope fractionation during microbially stimulated Fe(II) oxidation and Fe(II) precipitation. *Geochim Cosmochim Acta* 70:622–639
- Balistrieri LS, Borrok DM, Wanty RB, Ridley WI (2008) Fractionation of Cu and Zn isotopes during adsorption onto amorphous Fe(III) oxides: experimental mixing of acid rock drainage and pristine river water. *Geochim Cosmochim Acta* 72:311–328
- Barling J, Anbar AD (2004) Molybdenum isotope fractionation during adsorption by manganese oxides. *Earth Planet Sci Lett* 217:315–329
- Barling J, Arnold GL, Anbar AD (2001) Natural mass-dependent variations in the isotopic composition of molybdenum. *Earth Planet Sci Lett* 193:447–457
- Beard BL, Johnson CM (1999) High precision iron isotope measurements of terrestrial and lunar materials. *Geochim Cosmochim Acta* 63:1653–1660
- Beard BL, Johnson CM, Cox L, Sun H, Nealson KH, Aguilar C (1999) Iron isotope biosignatures. *Science* 285:1889–1892
- Beard BL, Johnson CM, Skulan JL, Nealson KH, Cox L, Sun H (2003) Application of Fe isotopes to tracing the geochemical and biological cycling of Fe. *Chem Geol* 195:87–117
- Beard BL, Handler RM, Scherer MM, Wu L, Czaja AD, Heimann A, Johnson CM (2010) Iron isotope fractionation between aqueous ferrous iron and goethite. *Earth Planet Sci Lett* 295:241–250
- Bergquist BA, Blum JD (2007) Mass-dependent and –independent fractionation of Hg isotopes by photoreduction in aquatic systems. *Science* 318:417–420
- Bergquist BA, Blum JD (2009) The odds and evens of mercury isotopes: applications of mass-dependent and mass-independent isotope fractionation. *Elements* 5:353–357
- Bermin J, Vance D, Archer C, Statham PJ (2006) The determination of the isotopic composition of Cu and Zn in seawater. *Chem Geol* 226:280–297
- Berna EC, Johnson TM, Makdisi RS, Basu A (2010) Cr stable isotopes as indicators of Cr(VI) reduction in groundwater: a detailed time-series study of a point-source plume. *Environ Sci Technol* 44:1043–1048
- Blum JD (2011) Applications of stable mercury isotopes to biogeochemistry. In: Baskaran M (ed) *Handbook of Environmental Isotope Geochemistry, Advances in Isotope Geochemistry*, DOI:10.1007/978-3-642-10637-8_10, © Springer-Verlag Berlin Heidelberg 2011
- Blum JD, Bergquist BA (2007) Reporting of variations in the natural isotopic composition of mercury. *Anal Bioanal Chem* 388:353–359
- Borrok DM, Wanty RB, Ridley WI, Wolf R, Lamothe PJ, Adams M (2007) Separation of copper, iron and zinc from complex aqueous solutions for isotopic measurement. *Chem Geol* 242:400–414
- Borrok DM, Nimick DA, Wanty RB, Ridley WI (2008) Isotopic variations of dissolved copper and zinc in stream waters affected by historical mining. *Geochim Cosmochim Acta* 72:329–344
- Briat JF, Curie C, Gaymard F (2007) Iron utilization and metabolism in plants. *Curr Opin Plant Biol* 10:276–282
- Bullen TD (2007) Chromium stable isotopes as a new tool for forensic hydrology at sites contaminated with anthropogenic chromium. In: Bullen TD, Wang Y (eds) *Water-rock interaction: proceedings of the 12th international symposium on water-rock interaction*, vol 1. Taylor & Francis, London, pp 699–702
- Bullen TD, Amundson R (2010) Interpreting Ca and Fe stable isotope signals in carbonates: a new perspective. *Proceedings of the 13th International Symposium on Water-Rock Interaction (WRI-13)*, Guanajuato, Mexico. Taylor & Francis, London
- Bullen TD, Eisenhauer AE (2009) Metal stable isotopes in low-temperature systems: a primer. *Elements* 5:349–352
- Bullen TD, Walczyk T (2009) Environmental and biomedical applications of natural metal stable isotope variations. *Elements* 5:381–385
- Bullen TD, White AF, Childs CW, Vivit DV, Schulz MS (2001) Demonstration of significant abiotic iron isotope fractionation in nature. *Geology* 29:699–702
- Cameron V, Vance D, Archer C, House C (2009) A biomarker based on the stable isotopes of nickel. *Proc Natl Acad Sci* 106:10944–10948
- CH2MHill (2007) Groundwater background study report, Hinkley Compressor Station, Hinkley, California. Internal Report to Pacific Gas & Electric Corporation, February 2007
- Charlson DV, Shoemaker RC (2006) Evolution of iron acquisition in higher plants. *J Plant Nutr* 29:1109–1125
- Chen JB, Gaillardet J, Louvat P (2008) Zinc isotopes in the Seine River waters, France: a probe of anthropogenic contamination. *Environ Sci Technol* 42:6494–6501
- Chen JB, Gaillardet J, Louvat P, Huon S (2009) Zinc isotopes in the suspended load of the Seine River, France: isotopic variations and source determination. *Geochim Cosmochim Acta* 73:4060–4076
- Clark I, Fritz P (1997) *Environmental isotopes in hydrogeology*. Lewis Publishers, Boca Raton, 328p
- Cloquet C, Carignan J, Libourel G, Sterckeman T, Perdrix E (2006a) Tracing source pollution in soils using cadmium and lead isotopes. *Environ Sci Technol* 40:2525–2530
- Cloquet C, Carignan J, Libourel G (2006b) Isotopic composition of Zn and Pb atmospheric depositions in an urban/periurban area of northeastern France. *Environ Sci Technol* 40: 6594–6600
- Cloquet C, Carignan J, Lehmann MF, Vanhaecke F (2008) Variation in the isotopic composition of zinc in the natural

- environment and the use of zinc isotopes in biogeosciences: a review. *Anal Bioanal Chem* 390:451–463
- Das J, Pobi M (1990) Separation of titanium, iron and aluminium on a chelating resin with benzoylphenylhydroxylamine group and application to bauxite and clay. *Fresenius' J Anal Chem* 336:578–581
- Eisenhauer A, Kisakurek B, Bohm F (2009) Marine calcification: an alkali earth metal isotope perspective. *Elements* 5: 365–368
- Ellis A, Johnson TM, Bullen TD (2002) Chromium isotopes and the fate of hexavalent chromium in the environment. *Science* 295:2060–2062
- Ellis A, Johnson TM, Bullen TD (2004) Using chromium stable isotope ratios to quantify Cr(VI) reduction: lack of sorption effects. *Environ Sci Technol* 38:3604–3607
- Estrade N, Carignan J, Sonke JE, Donard OFX (2009) Mercury isotope fractionation during liquid-vapor evaporation experiments. *Geochim Cosmochim Acta* 73:2693–2711
- Estrade N, Carignan J, Donard OFX (2010) Isotope tracing of atmospheric mercury sources in an urban area of northeastern France. *Environ Sci Technol* 44:6062–6067
- Fantle MS, Bullen TD (2009) Essentials of iron, chromium and calcium isotope analysis of natural materials by thermal ionization mass spectrometry. *Chem Geol* 258:50–64
- Geulke M, von Blanckenburg F (2007) Fractionation of stable iron isotopes in higher plants. *Environ Sci Technol* 41: 1896–1901
- Irisawa K, Hirata T (2006) Tungsten isotopic analysis of six geochemical reference materials using multiple collector-ICP-mass spectrometry coupled with rhenium-external correction technique. *Geochim Cosmochim Acta* 70:A279
- Izbicki JA, Ball JW, Bullen TD, Sutley SJ (2008) Chromium, chromium isotopes and selected trace elements, western Mojave Desert, USA. *Appl Geochim* 23:1325–1352
- Johnson TM (2011) Stable isotopes of Cr and Se as tracers of redox processes in earth surface environments. In: Baskaran M (ed) *Handbook of environmental isotope geochemistry*. Springer, Heidelberg
- Johnson CM, Beard BL (1999) Correction of instrumentally produced mass fractionation during isotopic analysis of Fe by thermal ionization mass spectrometry. *Int J Mass Spectrom* 193:87–99
- Johnson TM, Bullen TD, Zawislanski PT (2000) Selenium stable isotope ratios as indicators of sources and cycling of selenium: results from the northern reach of San Francisco Bay. *Environ Sci Technol* 34:2075–2079
- Johnson CM, Skulan JL, Beard BL, Sun H, Nealson KH, Braterman PS (2002) Isotopic fractionation between Fe(III) and Fe(II) in aqueous solutions. *Earth Planet Sci Lett* 195:141–153
- Johnson CM, Beard BL, Beukes NJ, Klein C, O'Leary JM (2003) Ancient geochemical cycling in the Earth as inferred from Fe isotope studies of banded iron formations from the Transvaal Craton. *Contrib Mineralog Petrol* 144: 523–547
- Johnson CM, Beard BL, Roden EE, Newman DK, Nealson KH (2004) Isotopic constraints on biogeochemical cycling of Fe. In: Johnson CM, Beard BL, Albarède F (eds) *Geochemistry of non-traditional stable isotopes*. Mineralogical Society of America Reviews in Mineralogy & Geochemistry 55: 359–408
- Johnson CM, Beard BL, Roden EE (2008) The iron isotope fingerprints of redox and biogeochemical cycling in modern and ancient Earth. *Annu Rev Earth Planet Sci* 36:457–493
- Kavner A, John SG, Sass S, Boyle EA (2008) Redox-driven stable isotope fractionation in transition metals: Application to Zn electroplating. *Geochim Cosmochim Acta* 72: 1731–1741
- Kendall C, McDonnell JJ (1998) Isotope tracers in catchment hydrology. Elsevier, Amsterdam, 839p
- Kiczka M, Wiederhold JG, Kraemer SM, Bourdon B, Kretzschmar R (2010) Iron isotope fractionation during Fe uptake and translocation in alpine plants. *Environ Sci Technol* 44: 6144–6150
- Kling GW, Evans WC, Tanyileke G, Kusakabe M, Ohba T, Yoshida Y, Hell JV (2005) Degassing Lakes Nyos and Monoun: defusing certain disaster. *Proc Natl Acad Sci USA* 102:14185–14190
- Kraemer SM, Crowley DE, Kretzschmar R (2006) Geochemical aspects of phytosiderophore-promoted iron acquisition by plants. *Adv Agron* 91:1–46
- Kramer U, Talke IN, Hanikenne M (2007) Transition metal transport. *FEBS Lett* 581:2263–2272
- Larson PB, Maher K, Ramos FC, Chang Z, Gaspar M, Meinert LD (2003) Copper isotope ratios in magmatic and hydrothermal ore-forming environments. *Chem Geol* 201:337–350
- Liu Y, Huang M, Masuda A, Inoue M (1998) High-precision determination of osmium and rhenium isotope ratios by in situ oxygen isotope ratio correction using negative thermal ionization mass spectrometry. *Int J Mass Spectrom Ion Processes* 173:163–175
- Longerich HP, Fryer BJ, Strong DF (1987) Determination of lead isotope ratios by inductively coupled plasma-mass spectrometry (ICP-MS). *Spectrochimica Acta* 42B:39–48
- Luo Y, Dabek-Zlotorzynska E, Celo V, Muir DCG, Yang L (2010) Accurate and precise determination of silver isotope fractionation in environmental samples by multi-collector-ICPMS. *Anal Chem* 82:3922–3928
- Malinovsky D, Hammarlund D, Ilyashuk B, Martinsson O, Gelting J (2007) Variations in the isotopic composition of molybdenum in freshwater lake systems. *Chem Geol* 236: 181–198
- Maréchal CN, Télouk P, Albarède F (1999) Precise analysis of copper and zinc isotopic compositions by plasma-source mass spectrometry. *Chem Geol* 156:251–273
- Marschner H (1995) *Mineral nutrition of higher plants*, 2nd edn. Academic, London, p 889
- Martin JH and Fitzwater SE (1988) Iron-deficiency limits phytoplankton growth in the Northeast Pacific Subarctic. *Nature* 331:341–343
- Mathur R, Ruiz J, Titley S, Liermann L, Buss H, Brantley SL (2005) Cu isotopic fractionation in the supergene environment with and without bacteria. *Geochim Cosmochim Acta* 69:5233–5246
- Mattielli N, Petit JCJ, Deboudt K, Flament P, Perdrix E, Taillez A, Rimetz-Planchon J, Weis D (2009) Zn isotope study of atmospheric emissions and dry depositions within a 5 km radius of a Pb-Zn refinery. *Atmos Environ* 43:1265–1272
- Moynier F, Pichat S, Pons M-L, Fike D, Balter V, Albarède F (2008) Isotopic fractionation and transport mechanisms of Zn in plants. *Chem Geol* 267:125–130

- Neubert N, Nägler TF, Böttcher ME (2008) Sulfidity controls molybdenum isotope fractionation into euxinic sediments: evidence from the modern Black Sea. *Geology* 36:775–778
- Pelly IZ, Lipschutz ME, Balsiger H (1970) Vanadium isotopic composition and contents in chondrites. *Geochim Cosmochim Acta* 34:1033–1036
- Polyakov VB, Mineev SD (2000) The use of Mossbauer spectroscopy in stable isotope geochemistry. *Geochim Cosmochim Acta* 64:849–865
- Poulson RL, Siebert C, McManus J, Berelson WM (2006) Authigenic molybdenum isotope signatures in marine sediments. *Geology* 34:617–620
- Rehkämper M, Wombacher F, Aggarwal JK (2004) Stable isotope analysis by multiple collector ICP-MS. In: de Groot PA (ed) *Handbook of stable isotope analytical techniques*. Elsevier, Amsterdam, pp 692–725
- Rehkämper M, Wombacher F, Horner TJ, Xue Z (2011) Natural and anthropogenic Cd isotope variations. In: Baskaran M (ed) *Handbook of Environmental Isotope Geochemistry, Advances in Isotope Geochemistry*, DOI 10.1007/978-3-642-10637-8_10, © Springer-Verlag Berlin Heidelberg 2011
- Richter FM, Dauphas N, Teng F-Z (2009) Non-traditional fractionation of non-traditional isotopes: Evaporation, chemical diffusion and Soret diffusion. *Chem Geol* 258:92–103
- Ripperger S, Rehkämper M (2007) Precise determination of cadmium isotope fractionation in seawater by double-spike MC-ICPMS. *Geochim Cosmochim Acta* 71:631–642
- Romheld V, Marschner H (1986) Evidence for a specific uptake system for iron phytosiderophores in roots of grasses. *Plant Physiol* 80:175–180
- Rudge JF, Reynolds BC, Bourdon B (2009) The double spike toolbox. *Chem Geol* 265:420–431
- Sahoo YV, Nakai S, Ali A (2006) Modified ion exchange separation for tungsten isotopic measurements from kimberlite samples using multi-collector inductively coupled plasma mass spectrometry. *Analyst* 131:434–439
- Schauble EA (2003) Modeling zinc isotope fractionations. *EOS Trans AGU* 84:F232
- Schauble EA (2004) Applying stable isotope fractionation theory to new systems. In: Johnson CM, Beard BL, Albarède F (eds) *Geochemistry of non-traditional stable isotopes, reviews in mineralogy and geochemistry*, vol 55. Mineralogical Society of America and Geochemical Society, Washington, D.C., pp 65–111
- Schmitt A-D, Galer SJG, Abouchami W (2009a) High-precision cadmium stable isotope measurements by double spike thermal ionization mass spectrometry. *J Anal At Spectrom* 24:1079–1088
- Schmitt A-D, Galer SJG, Abouchami W (2009b) Mass-dependent cadmium isotopic variations in nature with emphasis on the marine environment. *Earth Planet Sci Lett* 277:262–272
- Schoenberg R, Zink S, Staubwasser M, von Blanckenburg F (2008) The stable Cr isotope inventory of solid Earth reservoirs determined by double spike MC-ICP-MS. *Chem Geol* 249:294–306
- Schroeder WH, Munthe J (1998) Atmospheric mercury – an overview. *Atmos Environ* 32:809–822
- Severmann S, Anbar AD (2009) Reconstructing paleoredox conditions through a multitracer approach: the key to the past is the present. *Elements* 5:359–364
- Severmann S, Lyons TW, Anbar A, McManus J, Gordon G (2008) Modern iron isotope perspective on the benthic iron shuttle and the redox evolution of ancient oceans. *Geology* 36:487–490
- Shiel AE, Weiss D, Orians KJ (2010) Evaluation of zinc, cadmium and lead isotope fractionation during smelting and refining. *Sci Total Environ* 408:2357–2368
- Siebert C, Nägler TF, Kramers JD (2001) Determination of molybdenum isotope fractionation by double-spike multicollector inductively coupled plasma mass spectrometry. *Geochem Geophys, Geosyst* 2:1032
- Siebert C, Nagler TF, von Blanckenburg F, Kramers JD (2003) Molybdenum isotope records as a potential new proxy for paleoceanography. *Earth Planet Sci Lett* 211:159–171
- Siebert C, McManus J, Bice A, Poulson R, Berelson WM (2006) Molybdenum isotope signatures in continental margin marine sediments. *Earth Planet Sci Lett* 241:723–733
- Sikora ER, Johnson TM, Bullen TD (2008) Microbial mass-dependent fractionation of chromium isotopes. *Geochim Cosmochim Acta* 72:3631–3641
- Sivry Y, Riotté J, Sonke JE, Audry S, Schäfer J, Viers J, Blanc G, Freydrich R, Dupré B (2008) Zn isotopes as tracers of anthropogenic pollution from Zn-ore smelters: the Rio Mort-Lot River system. *Chem Geol* 255:295–304
- Skulan JL, Beard BL, Johnson CM (2002) Kinetic and equilibrium Fe isotope fractionation between aqueous Fe(III) and hematite. *Geochim Cosmochim Acta* 66:2995–3015
- Suzuki M et al (2006) Biosynthesis and secretion of mugineic acid family phytosiderophores in zinc-deficient barley. *Plant J* 48:85–97
- Teutsch N, Schmid M, Muller B, Halliday AN, Burgmann H, Wehrli B (2009) Large iron isotope fractionation at the oxic-anoxic boundary in Lake Nyos. *Earth Planet Sci Lett* 285:52–60
- Thevenot DR, Moilleron R, Lestel L, Gromaire MC, Rocher V, Cambier P, Bonte P, Colin JL, de Ponteves C, Maybeck M (2007) Critical budget of metal sources and pathways in the Seine River basin (1994–2003) for Cd, Cr, Cu, Hg, Ni, Pb and Zn. *Sci Total Environ* 375:180–203
- Vance D, Archer C, Bermin J, Perkins J, Statham PJ, Lohan MC, Elwood MJ, Mills RA (2008) The copper isotope geochemistry of rivers and the oceans. *Earth Planet Sci Lett* 274:204–213
- Viers J, Oliva P, Nonell A, Gélabert A, Sonke JE, Freydrich R, Gainville R, Dupré B (2007) Evidence of Zn isotopic fractionation in a soil plant system of a pristine tropical watershed (Nsimi, Cameroon). *Chem Geol* 239:124–137
- Von Blanckenburg F, von Wirén N, Guelke M, Weiss DJ, Bullen TD (2009) Fractionation of metal stable isotopes by higher plants. *Elements* 5:375–380
- Wasylenski LE, Rolfe BA, Weeks CL, Spiro TG, Anbar AD (2008) Experimental investigation of the effects of temperature and ionic strength on Mo isotope fractionation during adsorption to manganese oxides. *Geochim Cosmochim Acta* 72:5997–6005
- Weber KA, Achenbach LA, Coates JD (2006) Microorganisms pumping iron: anaerobic microbial oxidation and reduction. *Nat Rev Microbiol* 4:752–764
- Weiss DJ, Mason TFD, Zhao FJ, Kirk GJD, Coles BJ, Horstwood MSA (2005) Isotopic discrimination of zinc in higher plants. *New Phytol* 165:703–710

- Weiss DJ, Rausch N, Mason TFD, Coles BJ, Wilkinson JJ, Ukonmaanaho L, Arnold T, Nieminen TM (2007) Atmospheric deposition and isotope biogeochemistry of zinc in ombrotrophic peat. *Geochim Cosmochim Acta* 71: 3498–3517
- Welch SA, Beard BL, Johnson CM, Braterman PS (2003) Kinetic and equilibrium Fe isotope fractionation between aqueous Fe(II) and Fe(III). *Geochim Cosmochim Acta* 67:4231–4250
- Wen H, Carignan J, Cloquet C, Zhu X, Zhang Y (2010) Isotopic delta values of molybdenum standard reference and prepared solutions measured by MC-ICP-MS: proposition for delta zero and secondary references. *J Anal At Spectrom* 25: 716–721
- Widory D, Petelet-Giraud E, LeBihan O, LeMoullec Y, Quetel C, Snell J, Van Bocxstaele M, Hure A, Canard E, Joos E, Forti L, Bullen T, Johnson T, Fiani E (2010) Metals in atmospheric particles: can isotopes help discriminate potential sources? *Atmospheric Pollution, Special Edition*:75–82
- Wieser ME, Schwieters JB (2005) The development of multiple collector mass spectrometry for isotope ratio measurements. *Int J Mass Spectrom* 242:97–115
- Wiesli RA, Beard BL, Johnson CM (2004) Experimental determination of Fe isotope fractionation between aqueous Fe(II), siderite and “green rust” in abiotic systems. *Chem Geol* 211:343–362
- Wombacher F, Rehkamper M, Mezger K, Munker C (2003) Stable isotope compositions of cadmium in geological materials and meteorites determined by multiple-collector ICPMS. *Geochim Cosmochim Acta* 67:4639–4654
- Zhu XK, Guo Y, Williams RJP, O’Nions RK, Matthews A, Belshaw NS, Canters GW, deWaal EC, Weser U, Burgess BK, Salvato B (2002) Mass fractionation processes of transition metal isotopes. *Earth Planet Sci Lett* 200:47–62